nProFit: A Modern Pipeline for Structural Analysis of Stellar Clusters in the Rubin Observatory Era

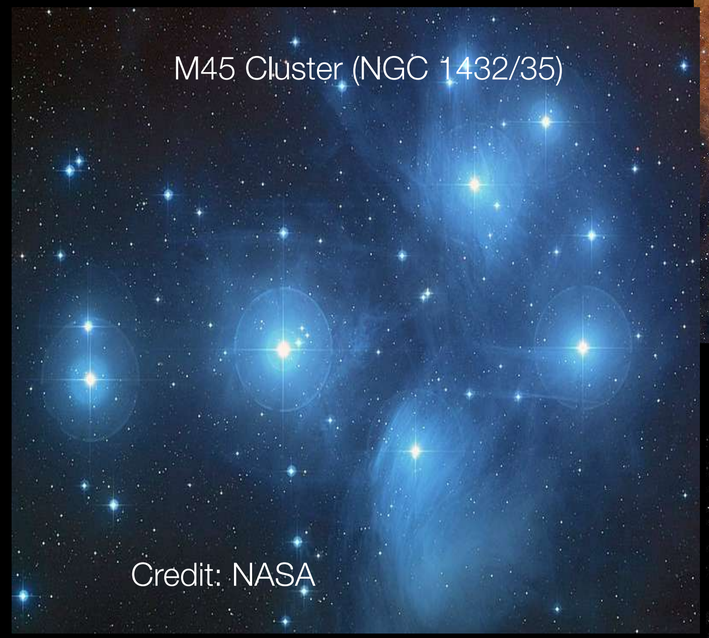
Bolivia Cuevas Otahola
Instituto de Astronomía
Universidad Nacional Autónoma de México

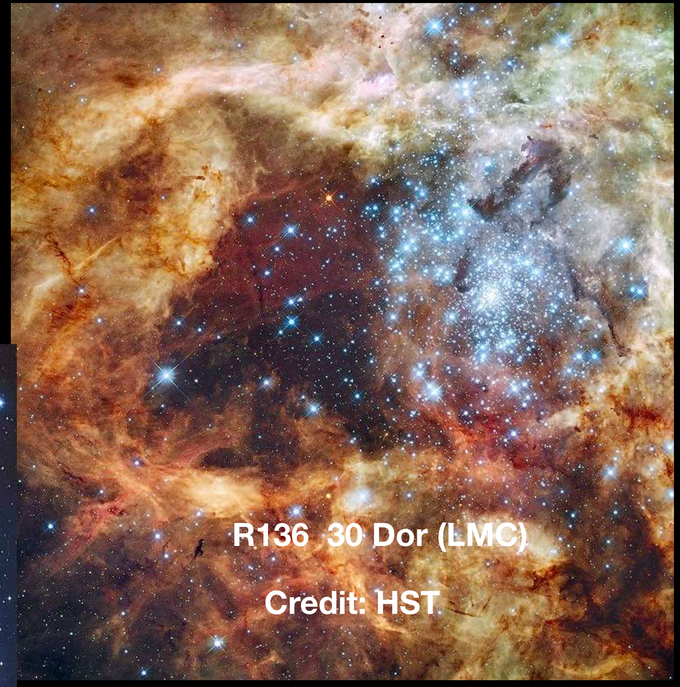


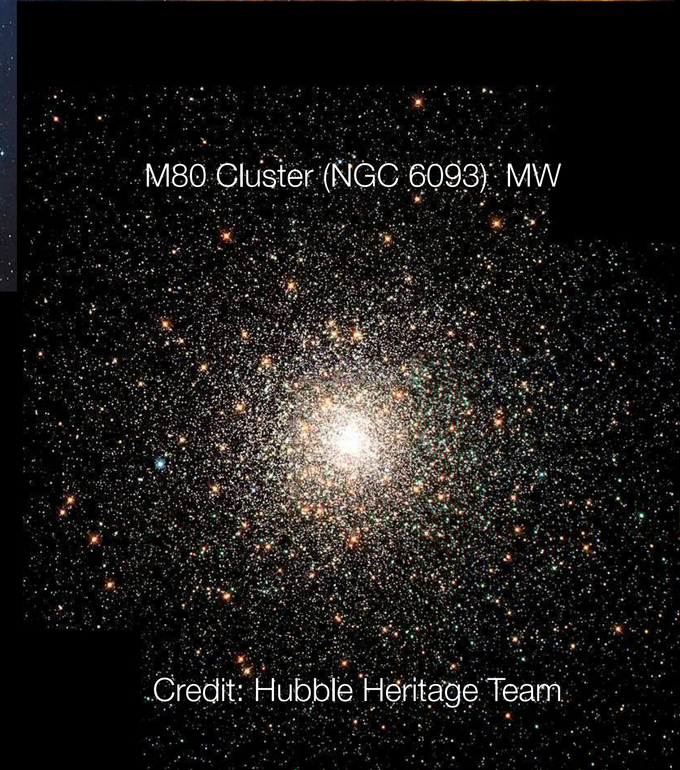
Star clusters

General properties

- Stars form in clusters
- Clusters are bound star associations
- Mass: $10^2\,M_\odot$ - $10^6\,M_\odot$
- ρ_0: 0.5 - $10^3\,M_\odot/pc^3$
- Sizes < 10 pc
- Ages:
  - ★ Young (<10 Myr)
  - ★ Intermediate-age (<1 Gyr)
  - ★ Old (>1 Gyr)







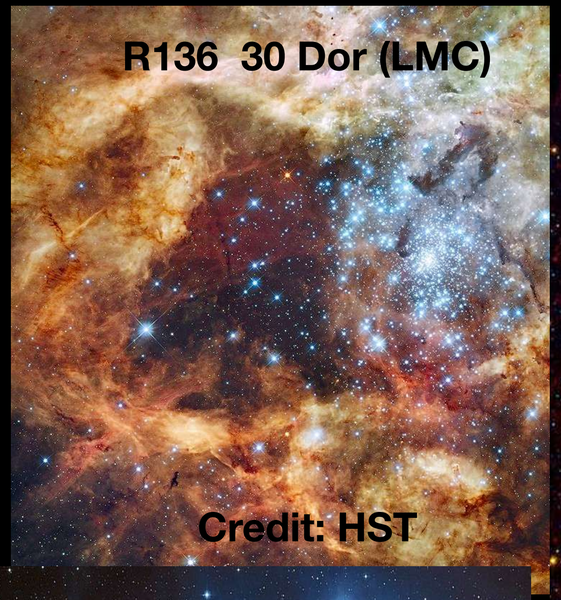
Why are super star clusters so important?

Star Clusters (SCs) relevance

- SCs are proxies of the chemical and dynamical evolution of their host galaxies.
- Young SCs are crucial to characterize the Cluster Initial Mass Function.
- SCs are natural laboratories to understand the evolution of variable stars and transients
- SSCs allow us to test the state-of-the art stellar evolution models.

Open Clusters (OCs)

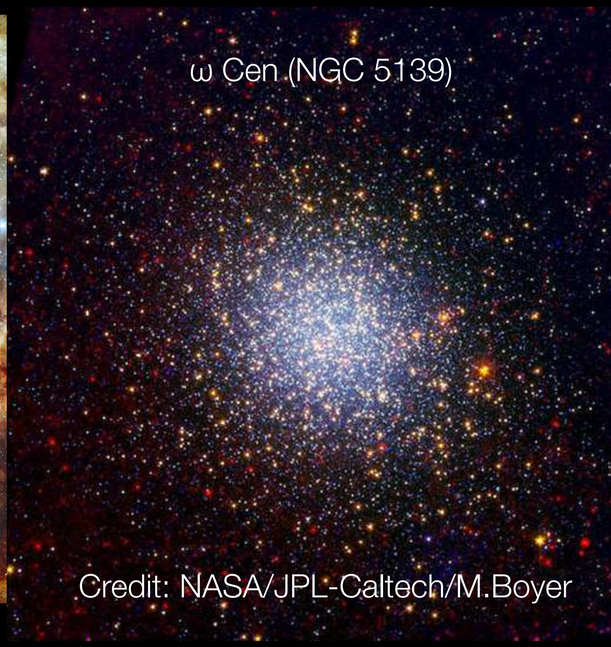
- Mass: 10^2 $M_\odot$- 10^3 $M_\odot$
- ρ_0: 0.1 - 10 $M_\odot/pc^3$
- r_h: ~10 pc





Globular clusters (GCs)

- Mass: 10^4 $M_\odot$- 10^6 $M_\odot$
- ρ_0: 0.5 - 10^3 $M_\odot/pc^3$
- r_h: ~3 pc



Super Star Clusters (SSCs)

- Mass: 10^4- 10^6 $M_\odot$ (Sharina 2016)
- ρ_0: >10^3 $M_\odot/pc^3$ (Portegies Zwart et al. 2010)
- r_h: 1-10 pc

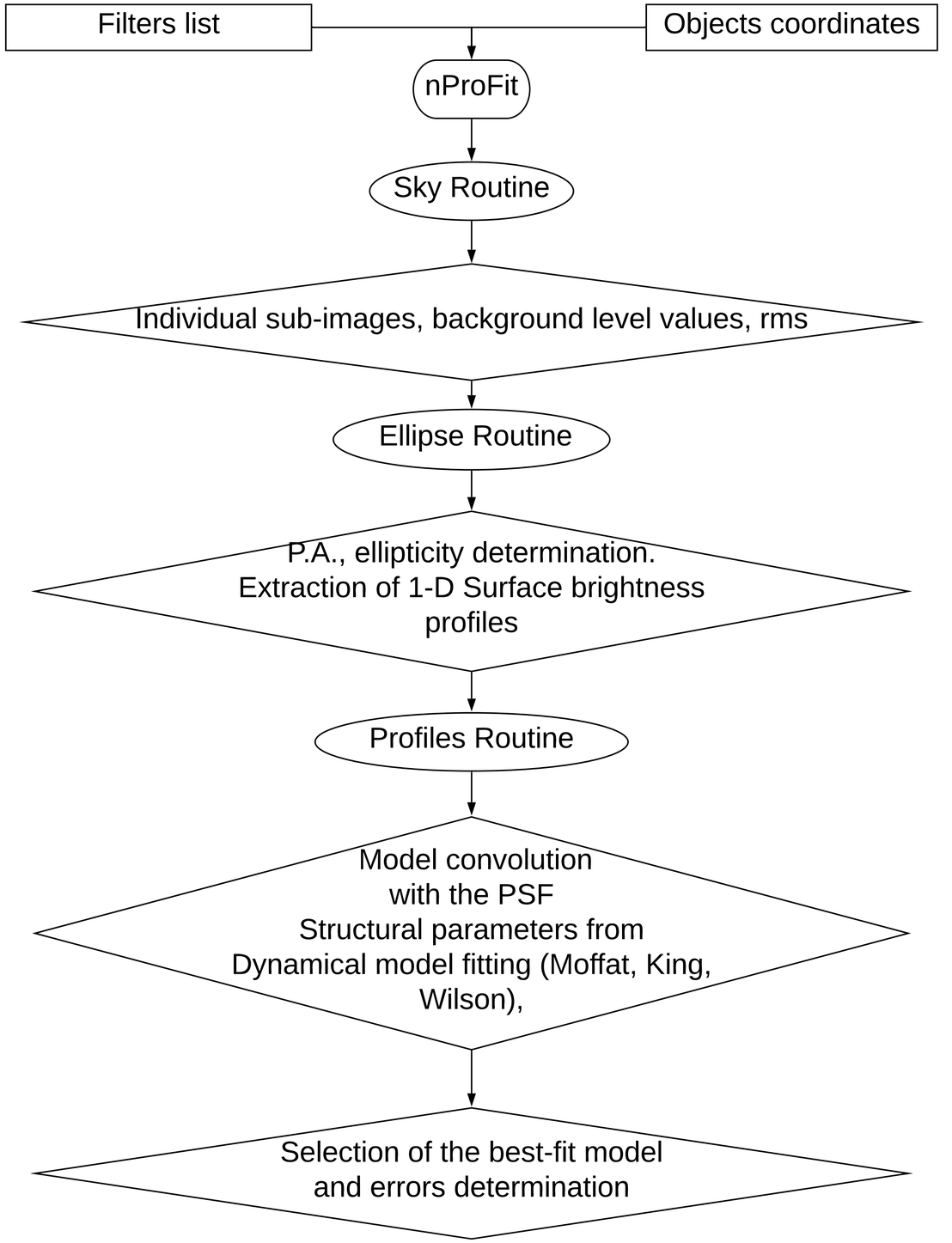
How do we obtain the structural parameters of star clusters?
The answer: **nProFit**

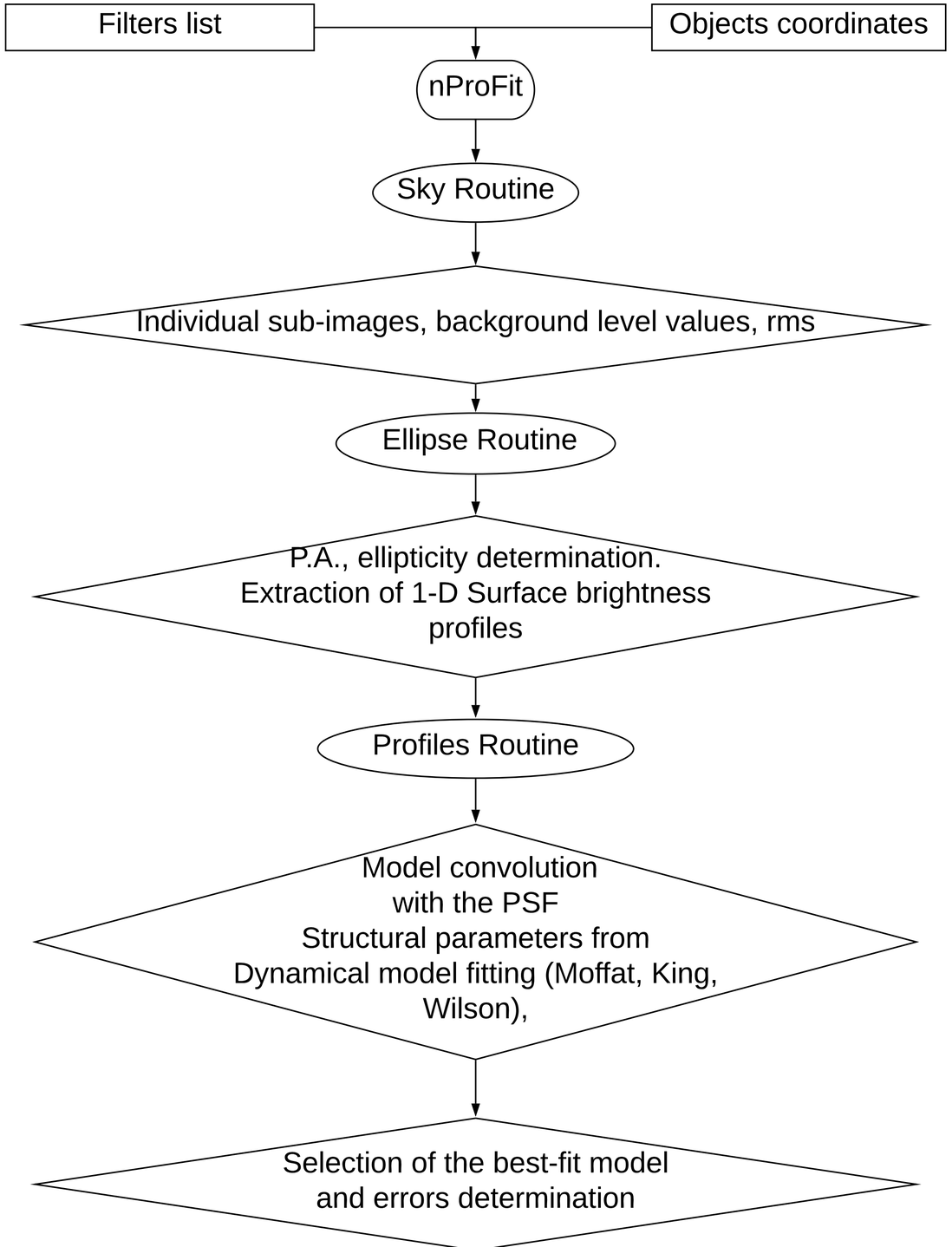
Obtaining structural parameters: n Profile Fitting tool: nProFit (Cuevas-Otahola et al. 2022)

nProFit (nProfile Fitting Tool) is a fitting tool implemented in PyRAF, Python and fortran, constituted by three main modules:

- Module to obtain sub-images centered in each object.
- Obtain and subtract Background and RMS level for each object.
- Obtain surface brightness profiles (SBPs).
- Determine the size and shape using PSF-convolved models.

Fully automated code providing the user with full control




Filters list
Objects coordinates
nProFit
Sky Routine
Individual sub-images, background level values, rms
Ellipse Routine
P.A., ellipticity determination.
Extraction of 1-D Surface brightness
profiles
Profiles Routine
Model convolution
with the PSF
Structural parameters from
Dynamical model fitting (Moffat, King,
Wilson),
Selection of the best-fit model
and errors determination

Filters list

Objects coordinates

nProFit

Sky Routine

Individual sub-images, background level values, rms

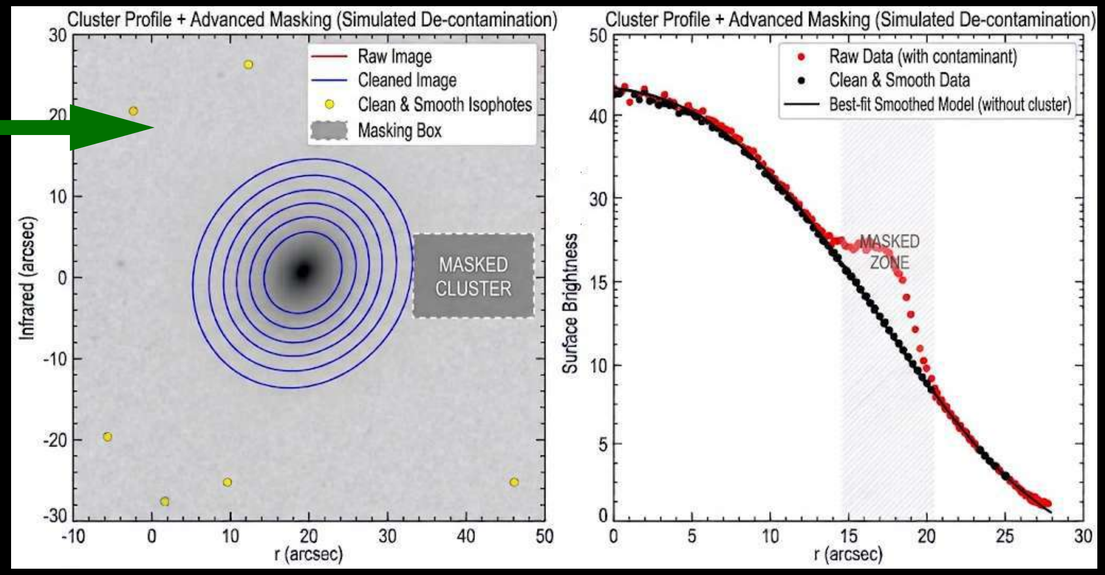
Ellipse Routine

P.A., ellipticity determination.
Extraction of 1-D Surface brightness profiles

Profiles Routine

Model convolution
with the PSF
Structural parameters from
Dynamical model fitting (Moffat, King, Wilson),

Selection of the best-fit model
and errors determination



Filters list

Objects coordinates

nProFit

Sky Routine

Individual sub-images, background level values, rms

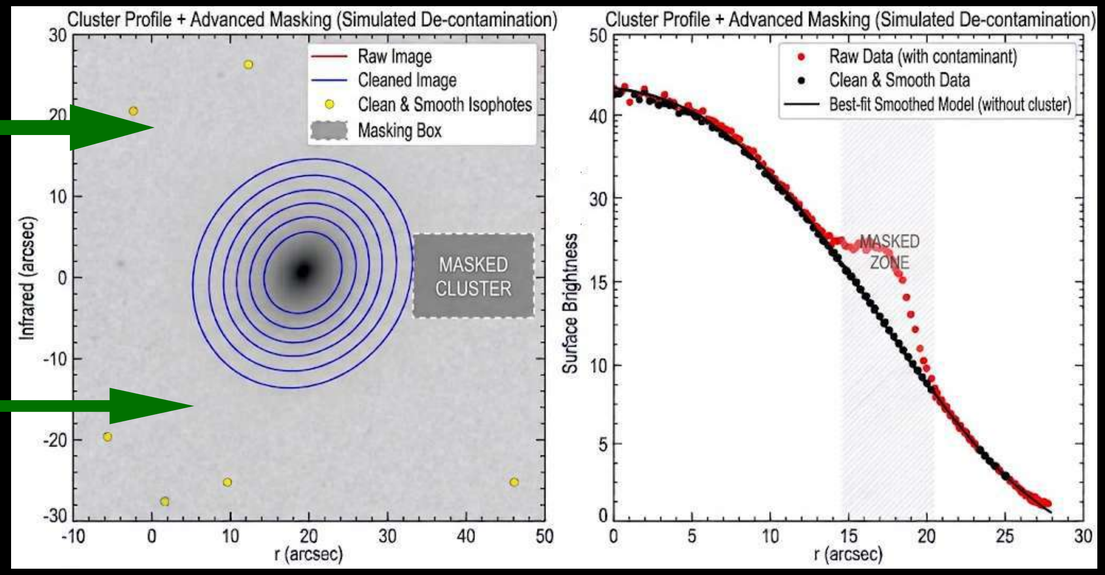
Ellipse Routine

P.A., ellipticity determination.
Extraction of 1-D Surface brightness profiles

Profiles Routine

Model convolution
with the PSF
Structural parameters from
Dynamical model fitting (Moffat, King, Wilson),

Selection of the best-fit model
and errors determination



Filters list

Objects coordinates

nProFit

Sky Routine

Individual sub-images, background level values, rms

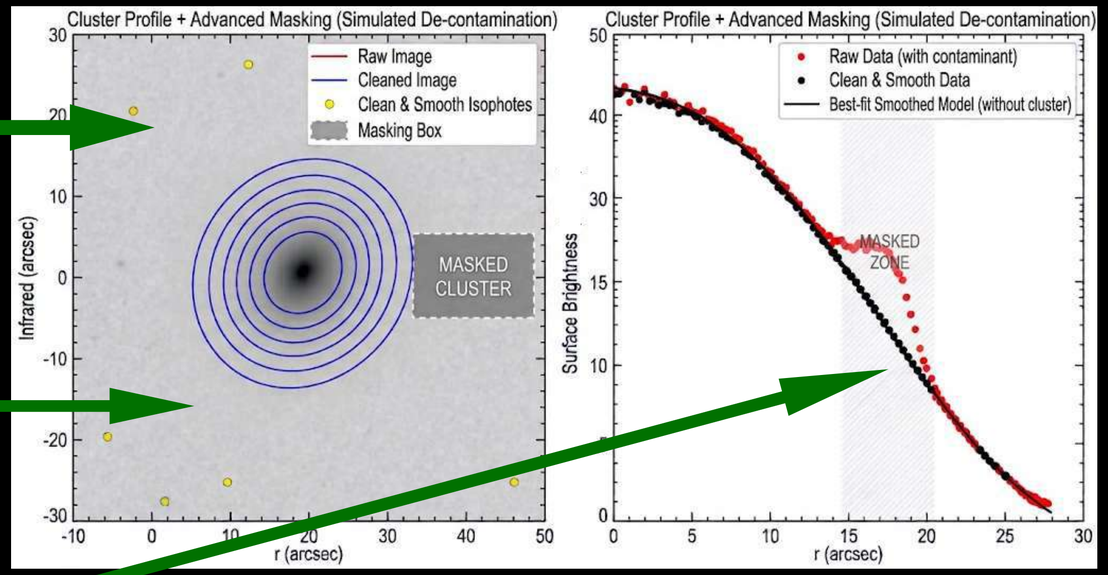
Ellipse Routine

P.A., ellipticity determination.
Extraction of 1-D Surface brightness profiles

Profiles Routine

Model convolution
with the PSF
Structural parameters from
Dynamical model fitting (Moffat, King, Wilson),

Selection of the best-fit model
and errors determination



Filters list

Objects coordinates

nProFit

Sky Routine

Individual sub-images, background level values, rms

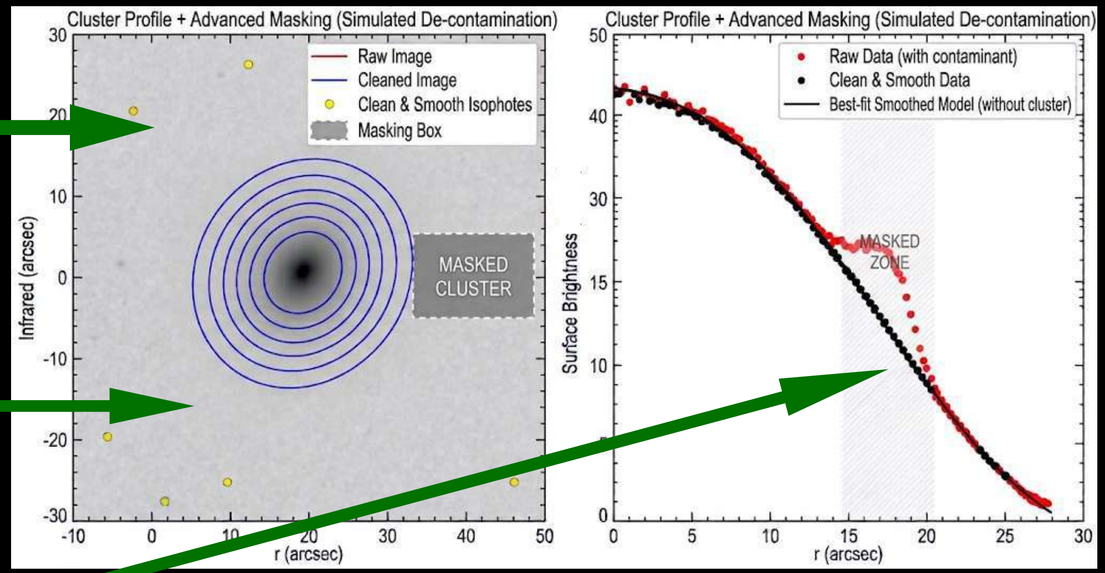
Ellipse Routine

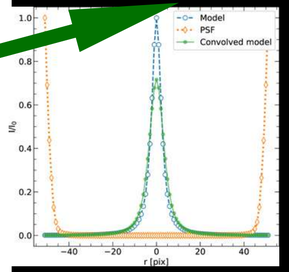
P.A., ellipticity determination.
Extraction of 1-D Surface brightness profiles

Profiles Routine

Model convolution with the PSF
Structural parameters from Dynamical model fitting (Moffat, King, Wilson),

Selection of the best-fit model and errors determination





Filters list

Objects coordinates

nProFit

Sky Routine

Individual sub-images, background level values, rms

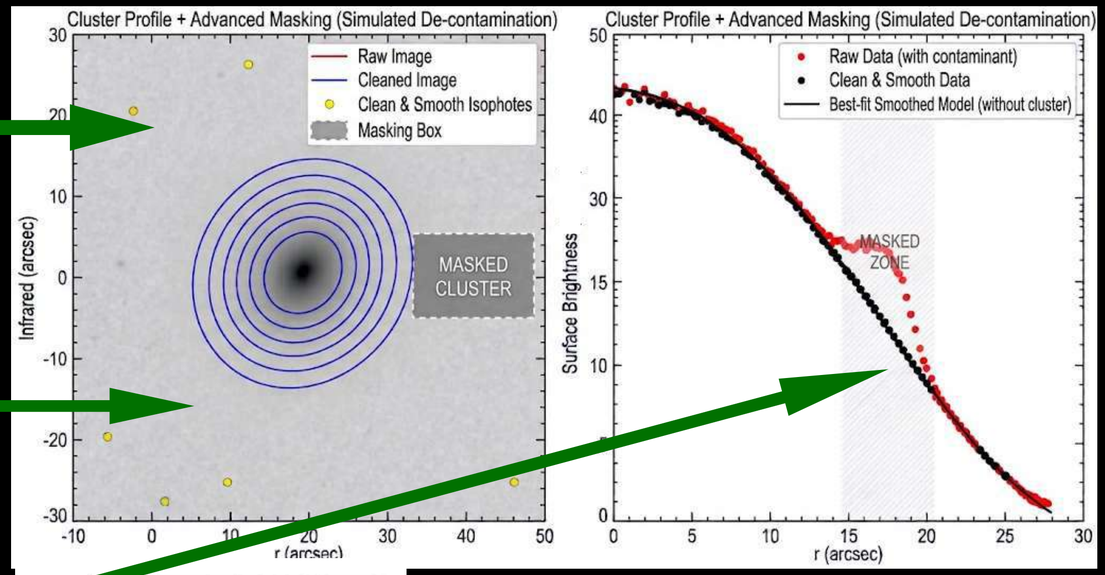
Ellipse Routine

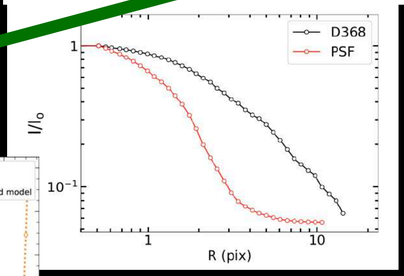
P.A., ellipticity determination.
Extraction of 1-D Surface brightness profiles

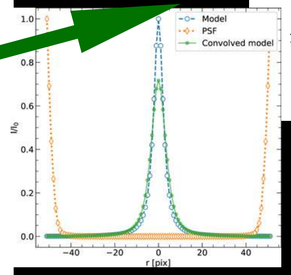
Profiles Routine

Model convolution with the PSF
Structural parameters from Dynamical model fitting (Moffat, King, Wilson),

Selection of the best-fit model and errors determination







Filters list

Objects coordinates

nProFit

Sky Routine

Individual sub-images, background level values, rms

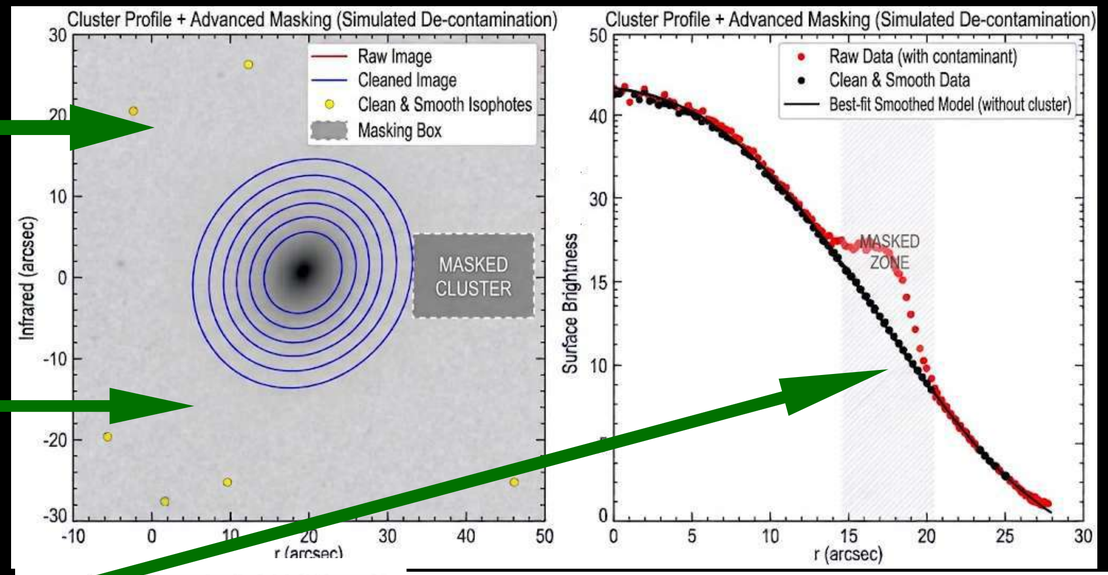
Ellipse Routine

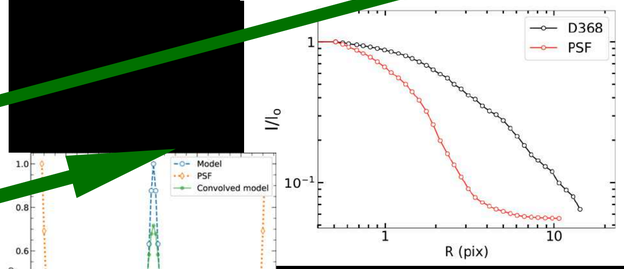
P.A., ellipticity determination.
Extraction of 1-D Surface brightness profiles

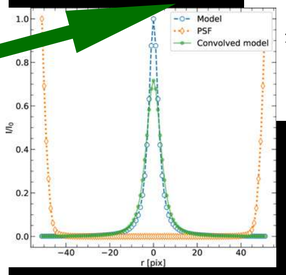
Profiles Routine

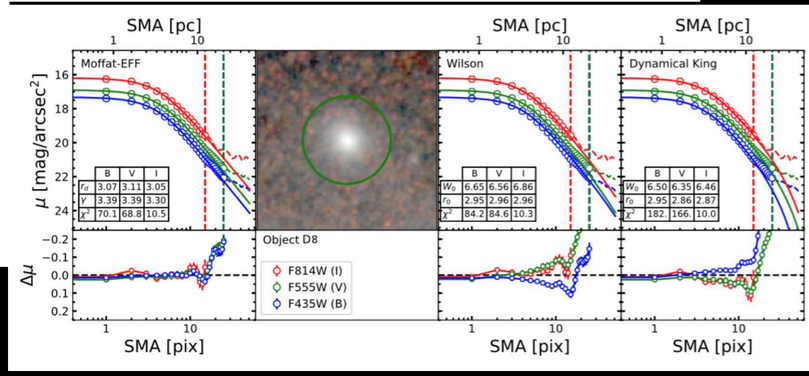
Model convolution with the PSF
Structural parameters from Dynamical model fitting (Moffat, King, Wilson),

Selection of the best-fit model and errors determination









Filters list

Objects coordinates

nProFit

Sky Routine

Individual sub-images, background level values, rms

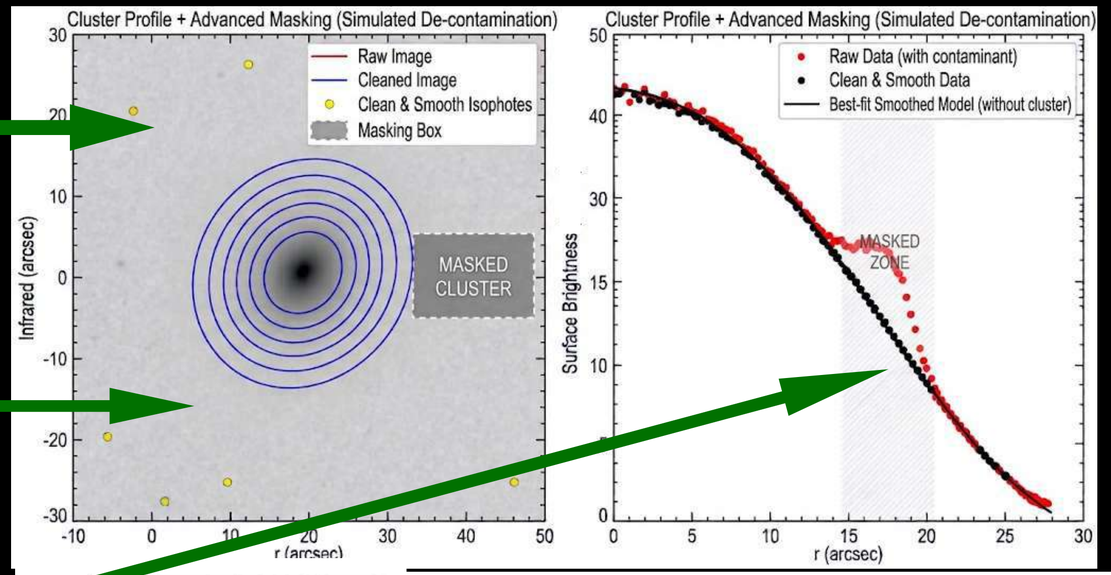
Ellipse Routine

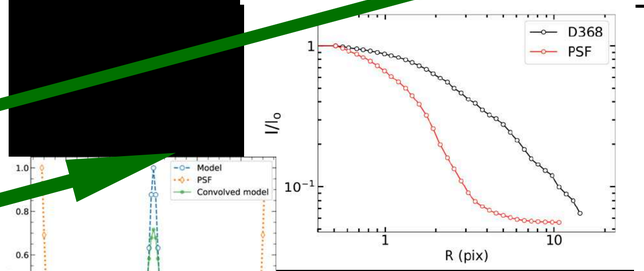
P.A., ellipticity determination.
Extraction of 1-D Surface brightness profiles

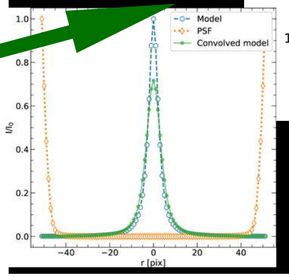
Profiles Routine

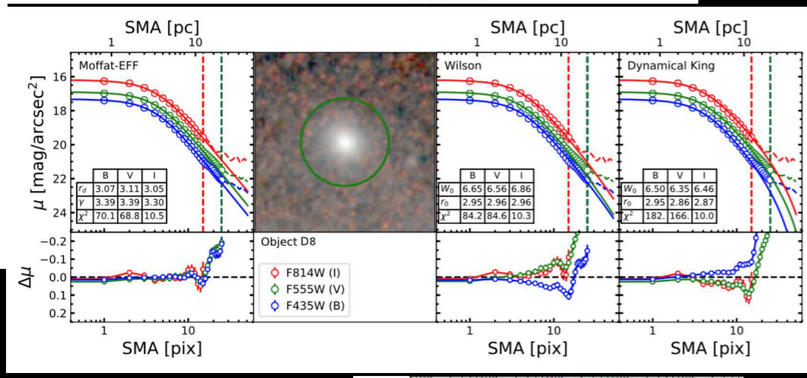
Model convolution
with the PSF
Structural parameters from
Dynamical model fitting (Moffat, King, Wilson),

Selection of the best-fit model
and errors determination

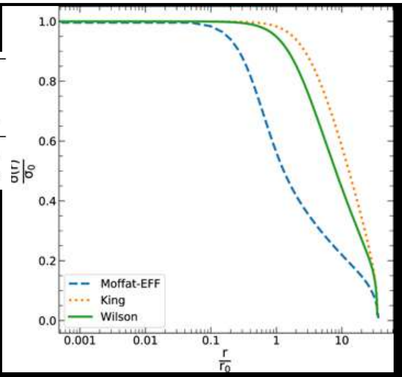








ID	R_g	γ	R_c	R_h	R_t	$\frac{M_b}{M}$	$\log(\rho_0)$	$\log(\Sigma_0)$	$\log(M)$	$\log(Ltot)$	$log(\rho_h)$	$log(I_h)$	$\sigma_{p,0}$	$\frac{R_{h,0}}{R_{j,0}}$
	(kpc)		(pc)	(pc)			($M_\odot/pc^3$)	($M_\odot/pc^2$)	($M_\odot$)	$L_\odot$	($M_\odot/pc^3$)	($L_\odot/pc^2$)	(km/s)	
(1)	(2)	(3)	(4)	(5)	(6)	(7)	(8)	(9)	(10)	(11)	(12)	(13)	(14)	(15)
D1	0.70	$2.73^{+0.04}_{-0.03}$	$0.57^{+0.05}_{-0.09}$	$1.67^{+0.15}_{-0.09}$	$31.67^{+0.29}_{-0.14}$	0.94	$4.99^{+0.04}_{-0.03}$	$5.06^{+0.19}_{-0.15}$	$5.68^{+0.28}_{-0.13}$	$6.57^{+0.28}_{-0.13}$	$4.39^{+0.06}_{-0.01}$	$5.32^{+0.06}_{-0.01}$	$13.35^{+0.29}_{-0.14}$	0.04
D8	2.61	$3.39^{+0.02}_{-0.02}$	$2.21^{+0.04}_{-0.04}$	$4.07^{+0.02}_{-0.02}$	$11.76^{+0.07}_{-0.07}$	0.85	$2.33^{+0.05}_{-0.05}$	$2.98^{+0.07}_{-0.07}$	$4.62^{+0.04}_{-0.04}$	$5.51^{+0.04}_{-0.04}$	$2.17^{+0.04}_{-0.04}$	$3.49^{+0.04}_{-0.04}$	$2.29^{+0.06}_{-0.06}$	0.06

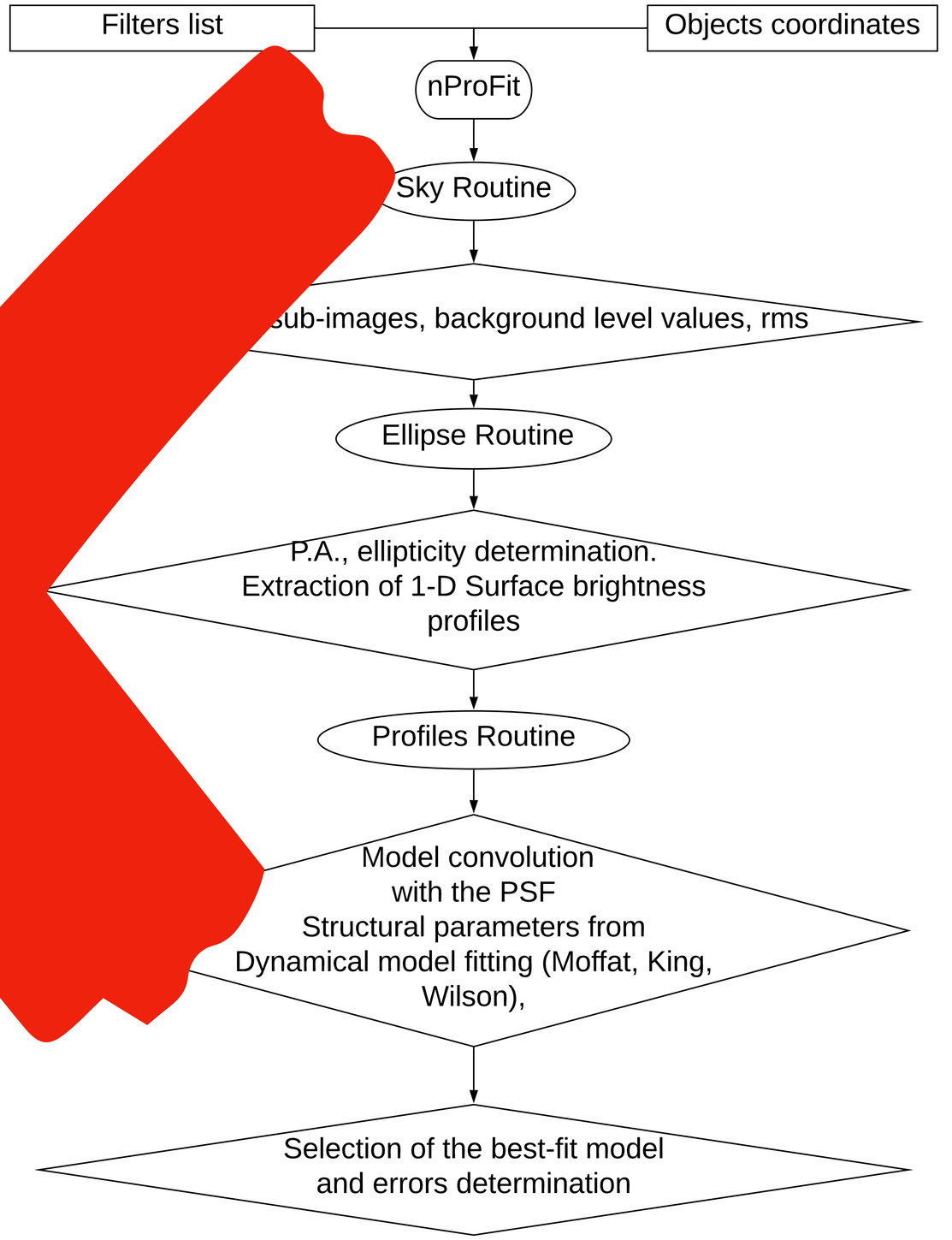


Obtaining structural parameters: n Profile Fitting tool: nProFit (Cuevas-Otahola et al.

nProFit (nProfile Fitting Tool) is a
implemented in PyRAF, Python a
constituted by three main modules:

- Module to obtain sub-images cente
each object.
- Obtain and subtract Background
level for each object.
- Obtain surface brightness pr
- Determine the size and s g PSF-
convolved models.

Fully automated code providing the user with full control



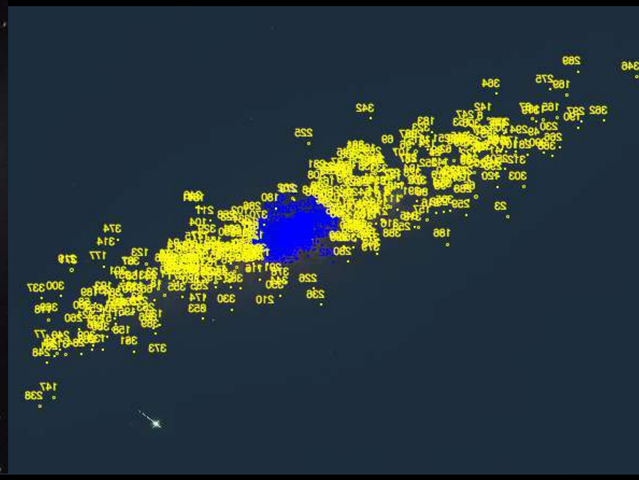
Rubin data requires a more robust and scalable approach: **nProFit new version**

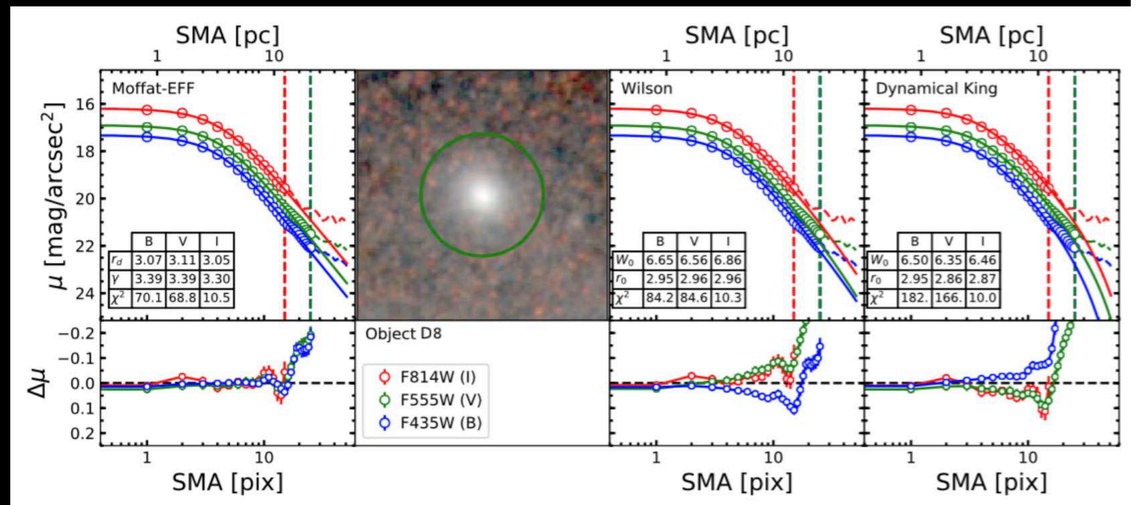
New LSST-related questions for nProFit

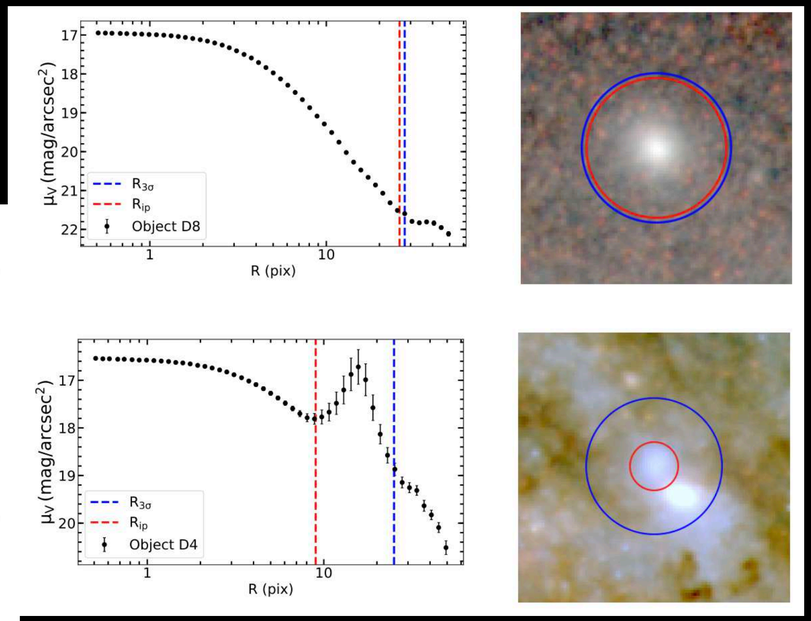
1. Which detections are genuine compact stellar systems?
2. What is their intrinsic structure after accounting for background, contamination, geometry, and the PSF?
3. How do size, concentration, truncation, and outer envelopes depend on environment and stellar population?



Credit: NASA, ESA, Hubble Heritage Team







New LSST-related questions for nProFit

1. Which detections are genuine compact stellar systems?

2. What is their intrinsic structure after accounting for background, contamination, geometry, and the PSF?

3. How do size, concentration, truncation, and outer envelopes depend on environment and stellar population?

New LSST-related questions for nProFit

1. Which detections are genuine compact stellar systems?

2. What is their intrinsic structure after accounting for background, contamination, geometry, and the PSF?

3. How do size, concentration, truncation, and outer envelopes depend on environment and stellar population?

New LSST-related questions for nProFit

1. Which detections are genuine compact stellar systems?
2. What is their intrinsic structure after accounting for background, contamination, geometry, and the PSF?
3. How do size, concentration, truncation, and outer envelopes depend on environment and stellar population?



- New segmentation technique

New LSST-related questions for nProFit

1. Which detections are genuine compact stellar systems?
2. What is their intrinsic structure after accounting for background, contamination, geometry, and the PSF?
3. How do size, concentration, truncation, and outer envelopes depend on environment and stellar population?

- New segmentation technique

New LSST-related questions for nProFit

1. Which detections are genuine compact stellar systems?
2. What is their intrinsic structure after accounting for background, contamination, geometry, and the PSF?
3. How do size, concentration, truncation, and outer envelopes depend on environment and stellar population?



- New segmentation technique



- New masking technique
- New PSF construction technique

New LSST-related questions for nProFit

1. Which detections are genuine compact stellar systems?
2. What is their intrinsic structure after accounting for background, contamination, geometry, and the PSF?
3. How do size, concentration, truncation, and outer envelopes depend on environment and stellar population?







- New segmentation technique
- New masking technique
- New PSF construction technique

New LSST-related questions for nProFit

1. Which detections are genuine compact stellar systems?
2. What is their intrinsic structure after accounting for background, contamination, geometry, and the PSF?
3. How do size, concentration, truncation, and outer envelopes depend on environment and stellar population?

- New segmentation technique
- New masking technique
- New PSF construction technique
- Revised dynamical models routines (multiplatform fortran support)

Target-specific segmentation and masking

Only reliable pixels contribute to the isophotal fit

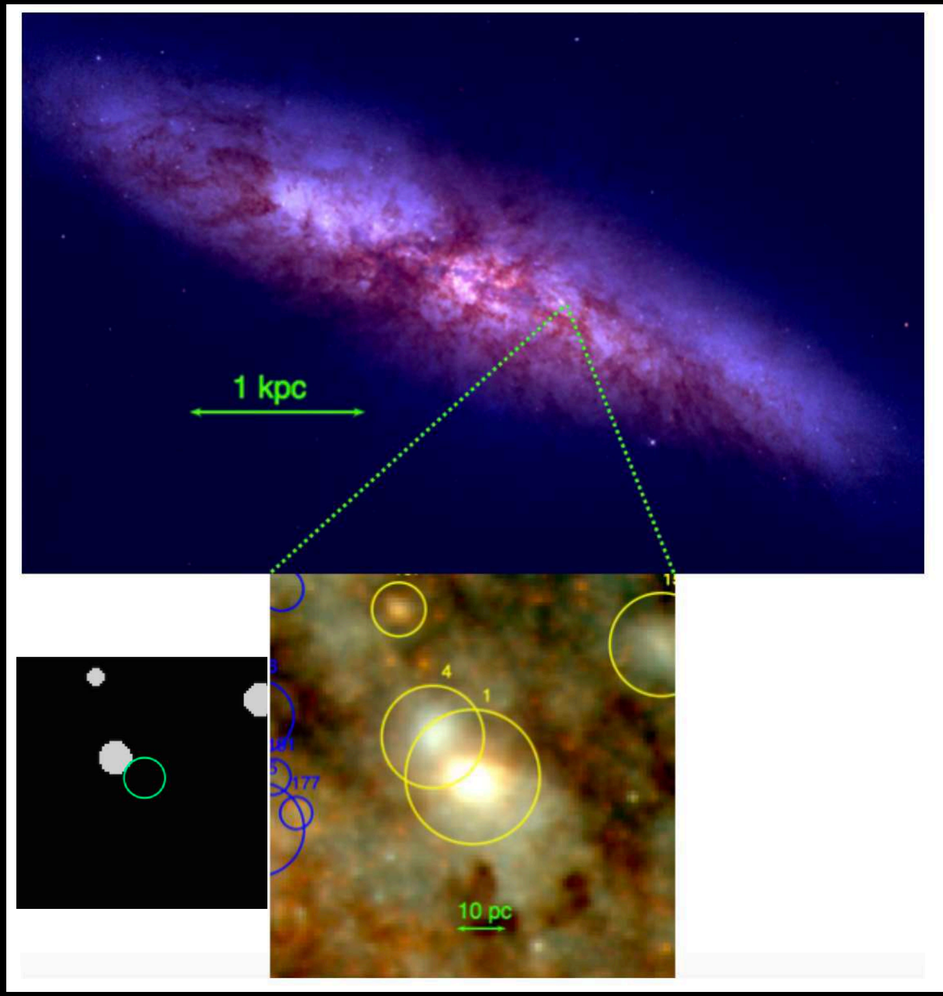
nProFit creates a High Pass image (I_{HP}) defined as

$$I_{HP} = I(x, y) - [G_{\sigma_{bkg}} \otimes I](x, y)$$

$I(x, y)$ is the original image

$G_{\sigma_{bkg}}$ a Gaussian kernel

I_{HP} preserves small-scale structures



Individual masks
Built from segmentation

From initial segmentation we have

$M_{neighbors}(x, y)$ from neighbouring sources

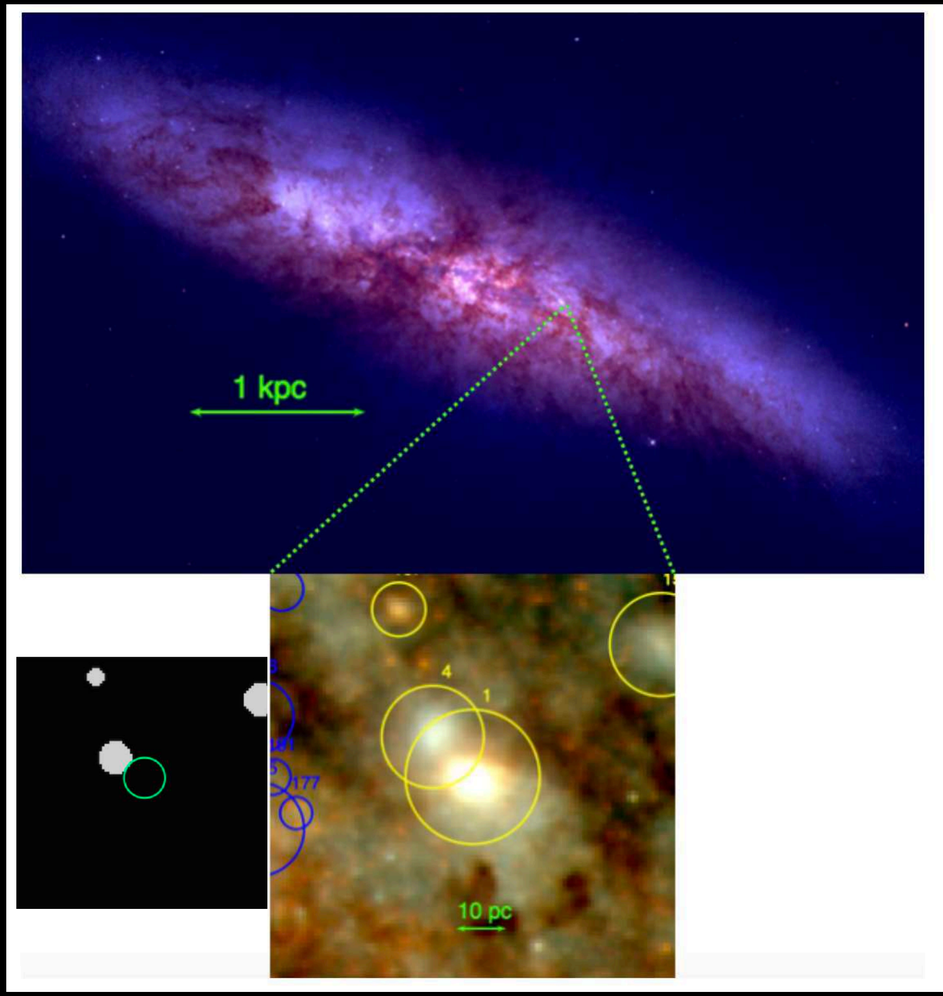
$M_{invalid}(x, y)$ NaN or invalid pixels

$M_{saturated}(x, y)$ saturated pixels

$M_{DQ}(x, y)$ rejected pixels according Data Quality flags (if available)

The combined masks are

$$M_{bad} = M_{neighbors} \vee M_{invalid} \vee M_{saturated} \vee M_{saturated}$$



PSF extraction

nProFit psf routine

- Initial PSF FWHM provided by the user
- Detect isolated stellar candidates
- Measure $\mathrm{FWHM_i}$ for each source
- Select the stellar FWHM locus
- Local-background subtraction
- + subpixel recentering
- + flux normalization

- Combine accepted stellar stamps
- Empirical PSF
- PSF-convolved cluster models

The stellar FWHM locus is given by

$$\mathrm{FWHM_{stellar}} = \mathrm{mode}(\mathrm{FWHM_1}, \cdots, \mathrm{FWHM_N})$$

$$\left| \frac{\mathrm{FWHM_i} - \mathrm{FWHM_{stellar}}}{\mathrm{FWHM_{stellar}}} \right| \leq 0.25$$

Coming up on late November:

nProFit 2.0
Mexican IDAC

- As part of UNAM S4 in-kind contribution nProFit will be available in the Mexican IDAC.
- All users are invited to reach out (bcuevas@astro.unam.mx)
- After the publication of nProFit 2.0 the code will be released publicly
- Please reach out if you'd like to use nProFit 2.0





LAMOD
LABORATORIO
DE MODELOS Y DATOS DE LA UNAM

Conclusions and next steps

nProFit 2.0 expands the analysis beyond profile fitting

- **Compact-source identification** on structured galactic backgrounds
- **Target-specific masks** for reliable isophotal profiles
- **Empirical PSF construction** from isolated field stars
- PSF-convolved Moffat-EFF, King, and Wilson models
- Reproducible, multiplatform structural analysis

Born Again in the LSST

Can Rubin's Legacy Survey of Space and Time find the next Sakurai's Object?



Steven Margheim

In-kind Program Coordinator, Rubin Observatory

NSF–DOE Vera C. Rubin Observatory · NSF NOIRLab · LSST@LATAM 3, 3 November 2026

A star that dies twice

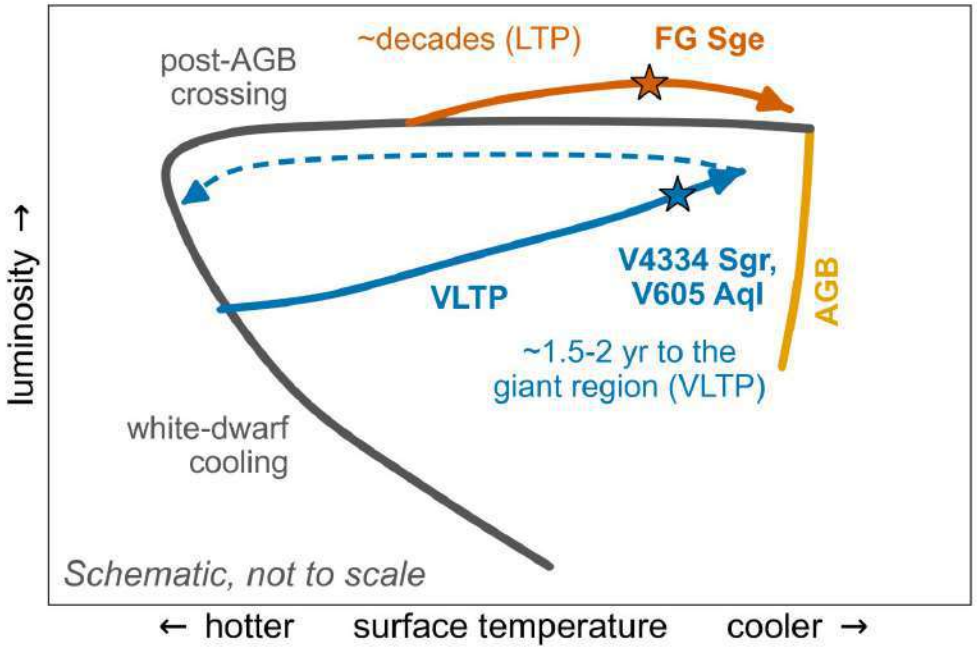
After the AGB, a star heads for the white-dwarf track.

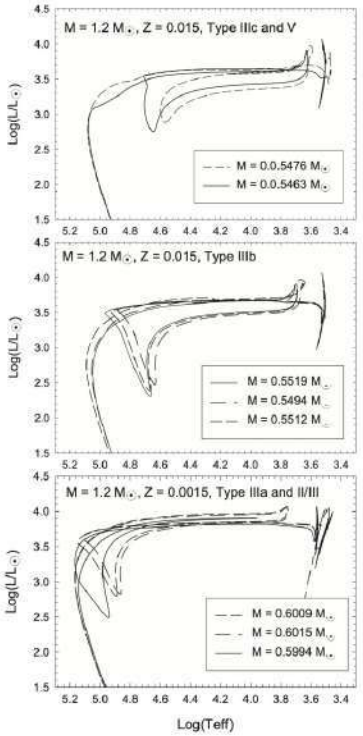
A few reignite helium in a late (LTP) or very late (VLTP) thermal pulse…

…and swell back into a cool, luminous, hydrogen-poor giant.

VLTP: ~1.5–2 years. LTP: decades.

Then dust forms and the star vanishes from the optical.



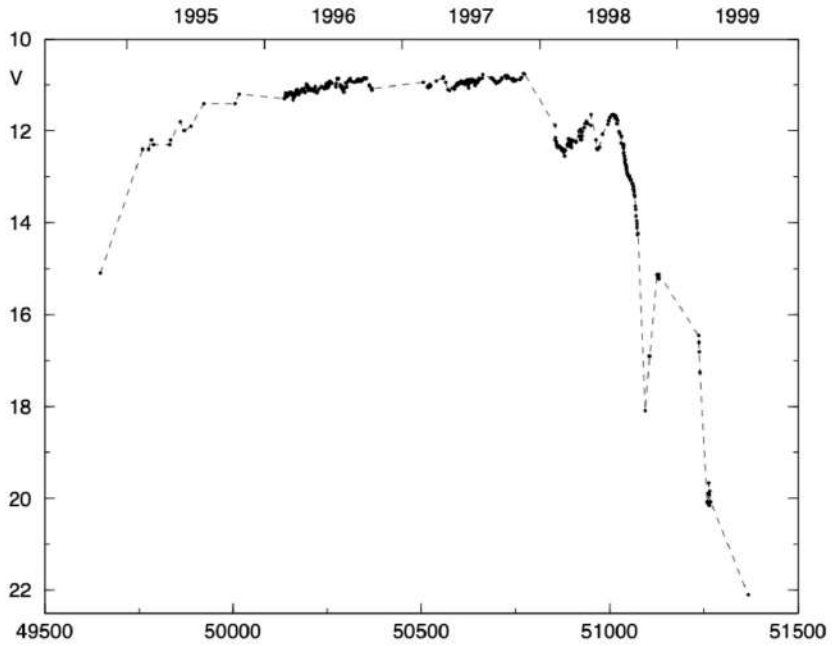


LTP models: Lawlor 2023, MNRAS 519, 5373, Fig. 2

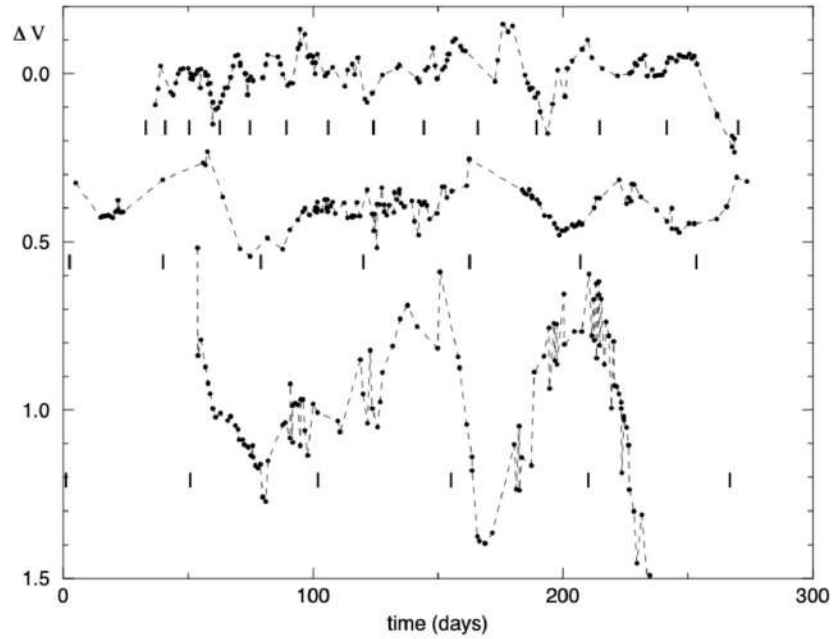
Only three seen in a century

Star	Pulse	What happened
V605 Aql	very late, 1917–19	Rose ~2 yr, dusty fades, gone by 1924
Sakurai's Object	very late, 1994–99	Rose ~1.5 yr; faded 11 mag into dust
FG Sge	late, 1894–present	Brightened over ~74 yr; R CrB-like fades since 1992

Sakurai's Object: a born-again star in fast forward



V light curve, 1995–1999 (Fig. 2)

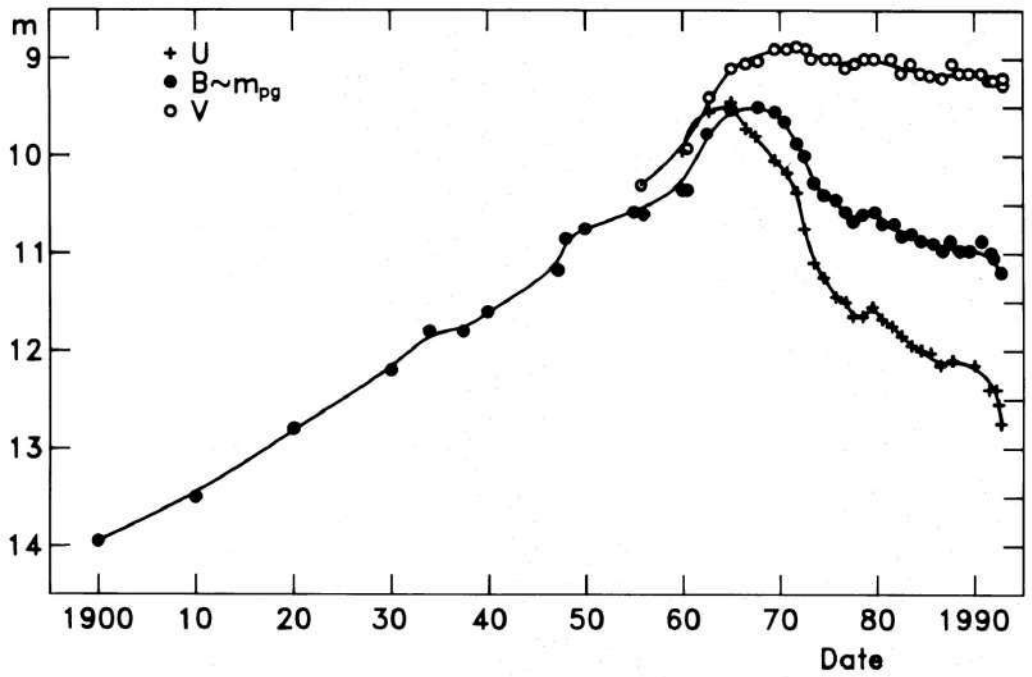


Plateau pulsations, detrended: 1996, 1997, 1998, top to bottom (Fig. 4)

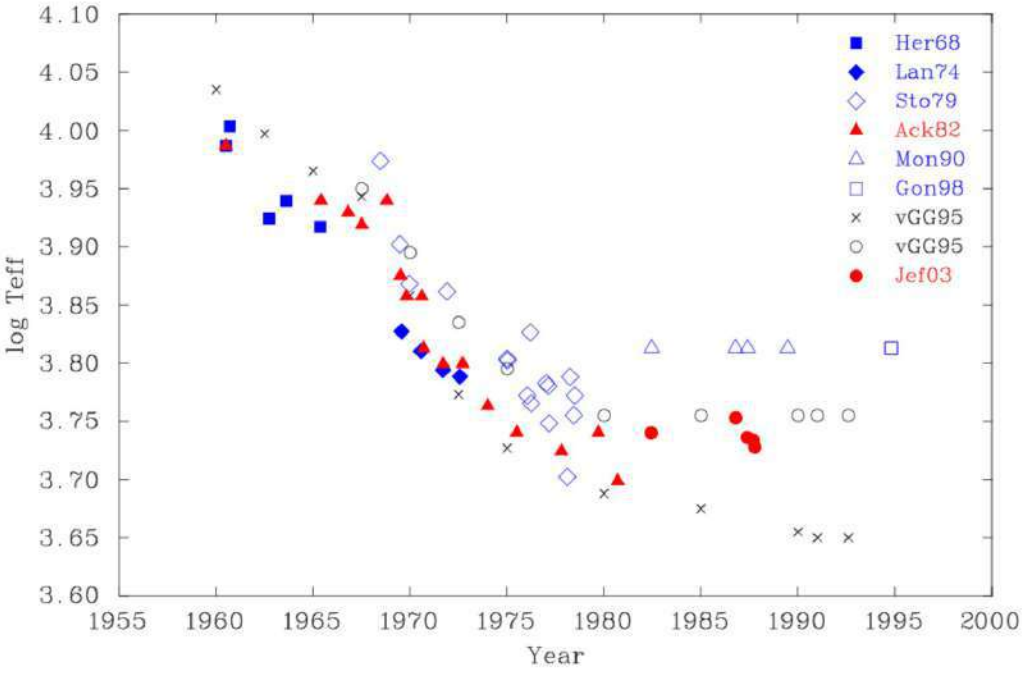
Both panels: Duerbeck et al. 2000, AJ 119, 2360

Rose to V ≈ 11 in ~1.5 yr; pulsations grew (≈ 56 → 74 d, 0.2 → 0.75 mag); then dust fades of 3–11 mag in 1998–99

FG Sge: a born-again star in slow motion



Brightness, 1900–1992 · van Genderen & Gautschy 1995, A&A 294, 453, Fig. 2



Temperature, 1960–1995 · Jeffery & Schönberner 2006, A&A 459, 885, Fig. 2

Brightened ~5 mag over ~74 years while cooling from ~10,000 K to ~5,000 K; R CrB-like dust fades since 1992

Models vs history

10–15%

of post-AGB stars have a very late pulse (models)

Lawlor & MacDonald 2003

~2 / yr

post-AGB stars born in the Milky Way

Moe & De Marco 2006

tens

of very late pulses expected per century

$10–15\% \times \sim 2\ \mathrm{yr}^{-1} \times 100\ \mathrm{yr} \approx 20–30$

…yet only ~2 noticed in the 20th century

V605 Aql 1919, Sakurai's Object 1996 (Duerbeck et al. 2002; Nakano 1996)

Either most are *missed*, or the models *over-predict*. LSST is deep, wide and long enough to tell which.

The project in four steps

1

How would the known events look to Rubin?

Move the three observed light curves to typical sightlines and compare with LSST's limits

Today → when, not if

2

A simple model: how many?

Birth rate × pulse fraction × time in LSST's window, pre-registered, with Monte Carlo ranges

Today → ~2 very late, ~5 late in 10 yr

3

A full model

Stellar population with 3D dust, LSST's real cadence, saturation, and the look-alikes

Next → yield, purity, completeness

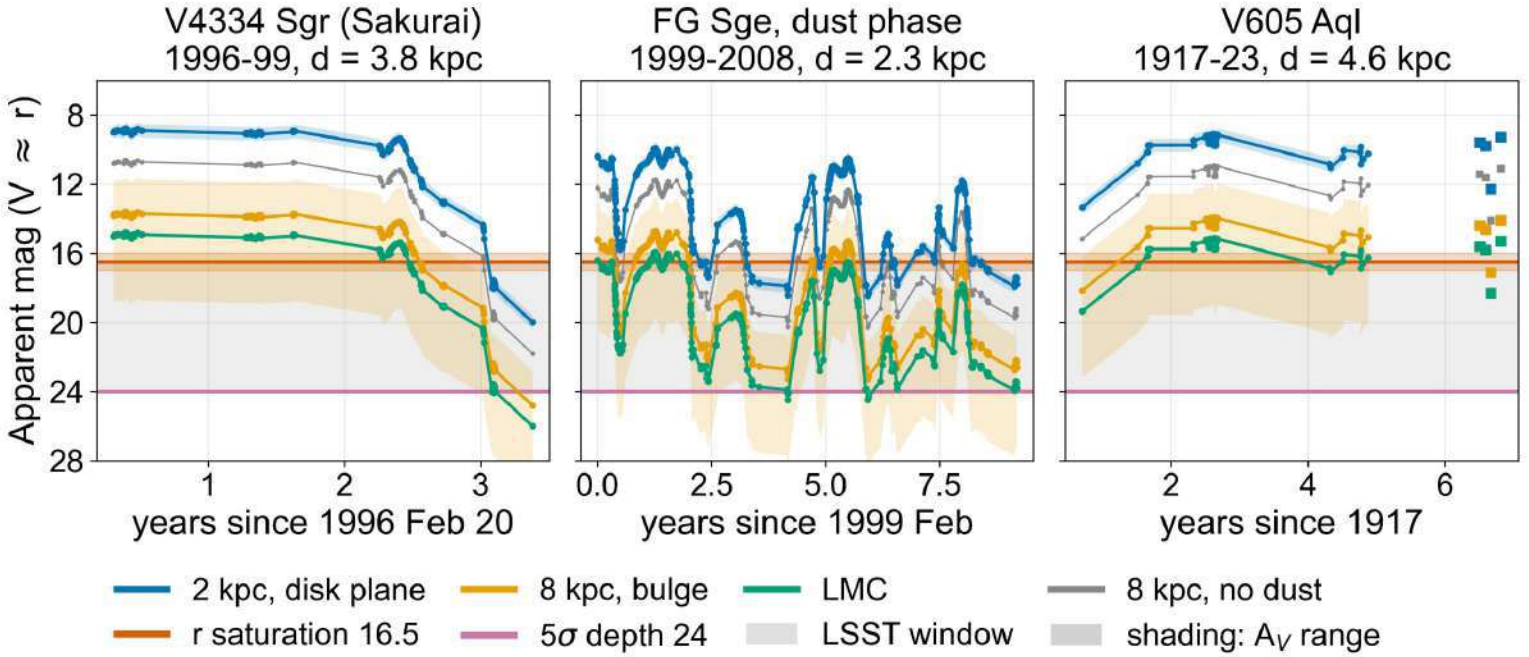
4

Detect them and tell them apart

Alert-stream and data-release filters, a planetary-nebula cross-match, follow-up spectra

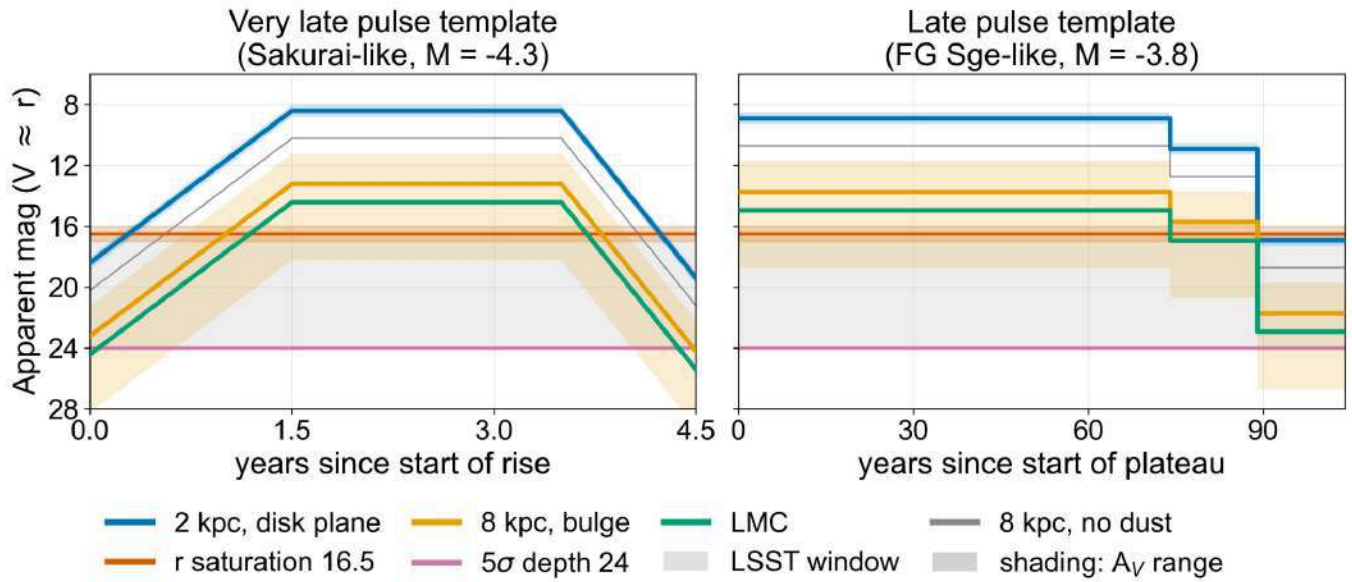
Next → a filter worth testing

How would the known events look to Rubin?



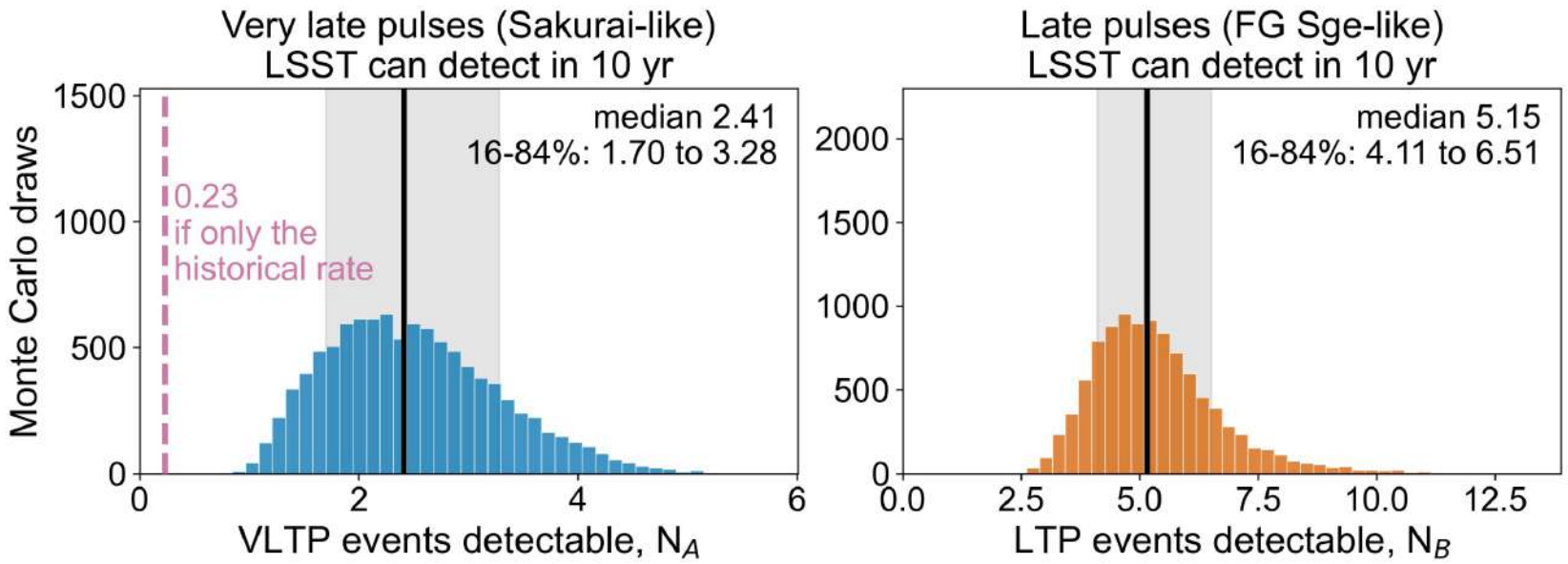
When, not if Too bright at peak, but **every event crosses LSST's window** on the rise and in the dust fade.

A pre-registered, order-of-magnitude estimate



1. N = Σ birth rate × pulse fraction × (time in LSST's window + 10 yr) × sky fraction
2. Thin and thick disk, bulge, halo, LMC, SMC; all inputs from the literature
3. Fixed and reviewed before any number was computed; 10,000 Monte Carlo draws

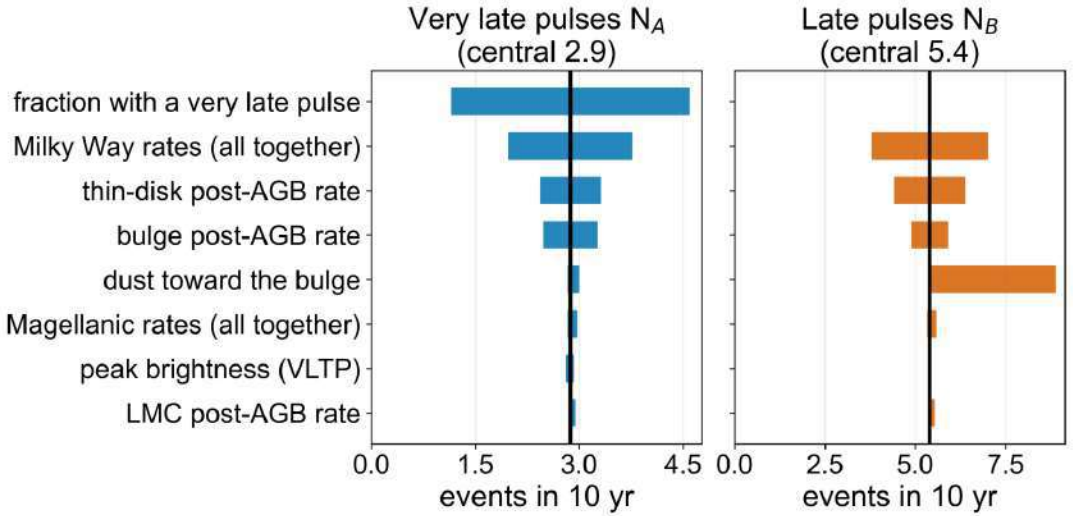
The answer: 2.4 very late and 5.2 late pulses



order-of-magnitude, pre-study estimate

91% chance of at least one very late pulse · ~10× the historical rate (0.23)

What drives it: how many happen, not LSST



The pulse fraction alone moves the very late count from **1.2 to 4.6**; saturation, depth, peak brightness and Galactic structure each change it by less than 10%.

Inputs: pulse fractions Lawlor & MacDonald 2003, Herwig 2001 · birth rates Moe & De Marco 2006, Reid & Parker 2006, Jacoby & De Marco 2002 · Galactic structure Girardi et al. 2005, Vanhollebeke et al. 2009, Bland-Hawthorn & Gerhard 2016, Jurić et al. 2008 · LSST limits LSST Science Collaboration 2009, Rubin key numbers · bulge dust A_V 1–8 mag (placeholder range)

Step 3: the full model

The early estimate assumed…	→ The full model will use…
A smooth Galaxy; bulge dust a guess (A_V 1–8)	A stellar population model with 3D dust maps, checked against planetary-nebula counts
Late pulses last 54–140 years	In models, the last cooling leg back to the giant branch alone takes 60–375 years (may raise the late-pulse count)
Time spent in LSST's window	Each event's simulated LSST visits; no alerts from saturated pixels; difference templates still building, completion uncertain
No look-alikes	R CrB stars, slow novae and others: how pure a selected sample can be

Step 3 delivers two products:

① A pre-LSST prediction, from current astrophysics, of how many LSST will detect

② Simulated LSST light curves of born-again stars and their look-alikes: the test bed for detection methods (step 4)

Step 4: finding them and telling them apart

Rise · 1–2 years

A steady brightening over months, often of a known planetary-nebula central star

Look for: a slow rise in the alerts' 12-month history, plus a planetary-nebula cross-match

→

Bright plateau

Usually too bright for LSST (only ~12% of very late peaks are unsaturated): hand off to other facilities for photometry and spectra

→

Dust fade

Looks like an R CrB star for ~2 years, then goes deeper and doesn't recover

Look for: the long light curve in the data releases

Why alerts? To get spectra early.

Sakurai's Object's first spectrum came a year into its rise, and its surface hydrogen then fell tenfold in six months. No very late pulse has spectroscopic coverage throughout its rise.

Next: build the full model; test a slow-rise filter on alerts against data-release light curves

Thank you!

¡Gracias! · Obrigado! · Questions?

When, not if: every known event crosses LSST's window

~2 very late, ~5 late pulses in 10 years (pre-study estimate)

Alerts → early spectra

This material is based upon work supported in part by the National Science Foundation through Cooperative Agreements AST-1258333 and AST-2241526 and Cooperative Support Agreements AST-1202910 and 2211468 managed by the Association of Universities for Research in Astronomy (AURA), and the Department of Energy under Contract No. DE-AC02-76SF00515 with the SLAC National Accelerator Laboratory managed by Stanford University. Additional Rubin Observatory funding comes from private donations, grants to universities, and in-kind support from LSST-DA Institutional Members. The work of S. Margheim is supported by NOIRLab, which is managed by the Association of Universities for Research in Astronomy (AURA) under a cooperative agreement with the U.S. National Science Foundation.

AI use: Anthropic Claude (5.x models) assisted with literature search, code, figures and drafting, under the author's direction; the author checked every number, source and figure. A log is kept with the project.



Caveats

- Detectable ≠ identified: R CrB stars (~350 in the Galaxy) fade the same way at first
- Bulge extinction is a placeholder range (A_V 1–8 mag); crude light-curve templates
- V treated as LSST r (no color term); LSST's on-sky bright limit not yet published
- Pulse fractions are model spreads, not measurement errors
- Detection modeled as brightness inside LSST's window, not as a change measured against the template

Inputs that drive the answer

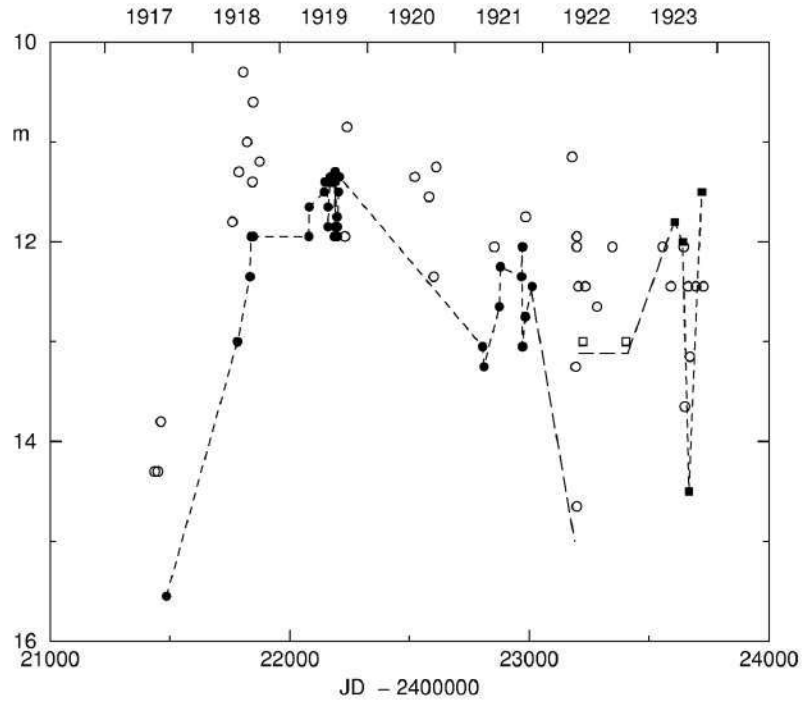
Input	Value (central; range)	Source
Post-AGB birth rate	Milky Way 2.0 yr^{-1}; LMC 0.047, SMC 0.011 yr^{-1}	Moe & De Marco 2006; Reid & Parker 2006; Jacoby & De Marco 2002
Very late pulse fraction	12.5% (5–20%, model spread)	Lawlor & MacDonald 2003; Herwig 2001
Late pulse fraction	7.5% (5–10%)	Herwig 2001
Peak brightness	M_V −4.3 (−3.0 to −5.4) very late; −3.8 late	Duerbeck et al. 2000; Clayton et al. 2013; Kimeswenger 2002

Sakurai's Object: identified in nine days, a year late

When	What happened
1995 January	Already 12.5 mag on patrol films: the rise is under way, unnoticed, with no spectrum
1996 Feb 20	Discovered by Yukio Sakurai as a "possible slow nova", 11.4 mag
Feb 23	First spectrum (ESO 3.6 m): a reddened, luminous early G-type star; no final flash suspected
Feb 24–25	Low-resolution spectra (ESO 1.52 m, $R \approx 2000$): carbon-rich, hydrogen-poor; first final-flash candidate since V605 Aql
Feb 29	A planetary nebula found around it
Apr–Oct 1996	Surface hydrogen falls tenfold; the earliest abundances were never measured

One spectrum plus a slow rise plus a nebula was enough, but only once someone looked

V605 Aql: Sakurai's older twin



Brightness, 1917–1923 · Duerbeck et al. 2002, Ap&SS 279, 183, Fig. 1

- Rose over ~2 years to a peak in mid-1919 (mpg ≈ 10.2 on the old scale, ≈ 11.3 recalibrated)
- Found by Max Wolf on 1919 Heidelberg plates; announced in 1920
- First spectrum in September 1921, two years after peak: a cool carbon star, like an R CrB star
- Three fades and recoveries in 1919–23, then gone; nothing seen to 16–17.5 mag in 1928–79
- Today: a hot Wolf-Rayet-type star (~95,000 K), V ≳ 23, inside the planetary nebula Abell 58

Which objects count as targets

- **Events:** very late and late pulses caught as they happen
- **Remnants:** central stars with observed evidence of a past pulse (5 confirmed: Sakurai's Object, A30, A58, A78, HuBi 1)
- **Context, labeled:** other hydrogen-poor central stars, AGB final pulses, merger products
- Bright remnants saturate in LSST; their signatures are spectroscopic

Recent survey candidates

- **ZTF:** two planetary-nebula central stars slowly brightening and reddening (CTSS 2, K 3-5), proposed late-pulse candidates
- **Archival:** IRAS 22568+6141 brightened ~1990 and has faded since; a possible late pulse
- Each has alternative readings (e.g., symbiotic star; shock or nova-like eruption)

Stars, Milky way & Local Volume Science Collaboration

Star Clusters Working Group

INSTITUTO DE ESTUDIOS ASTROFÍSICOS udp
FACULTAD DE INGENIERÍA Y CIENCIAS

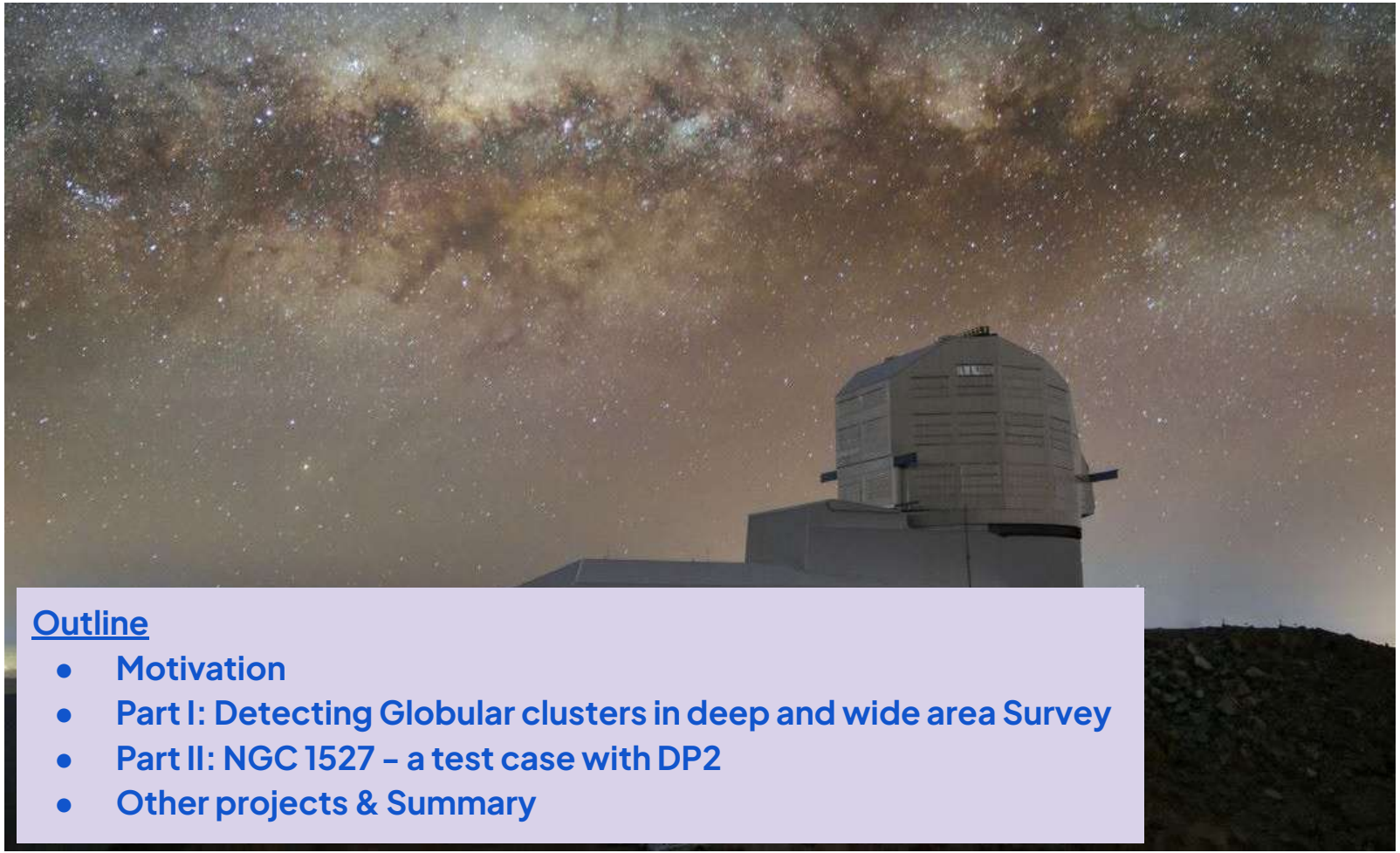
Tracing Galaxy Evolution with Rubin DP2 Photometry

A Combined Analysis of Integrated Light and Globular Cluster Systems

Yasna Ordenes-Briceño
Postdoctoral Researcher , Universidad Diego Portales, Chile.
Co-chair - Star Cluster Working Group SMWLV LSST SC.

LSST@LATAM, Sao Paulo
3rd November, 2026

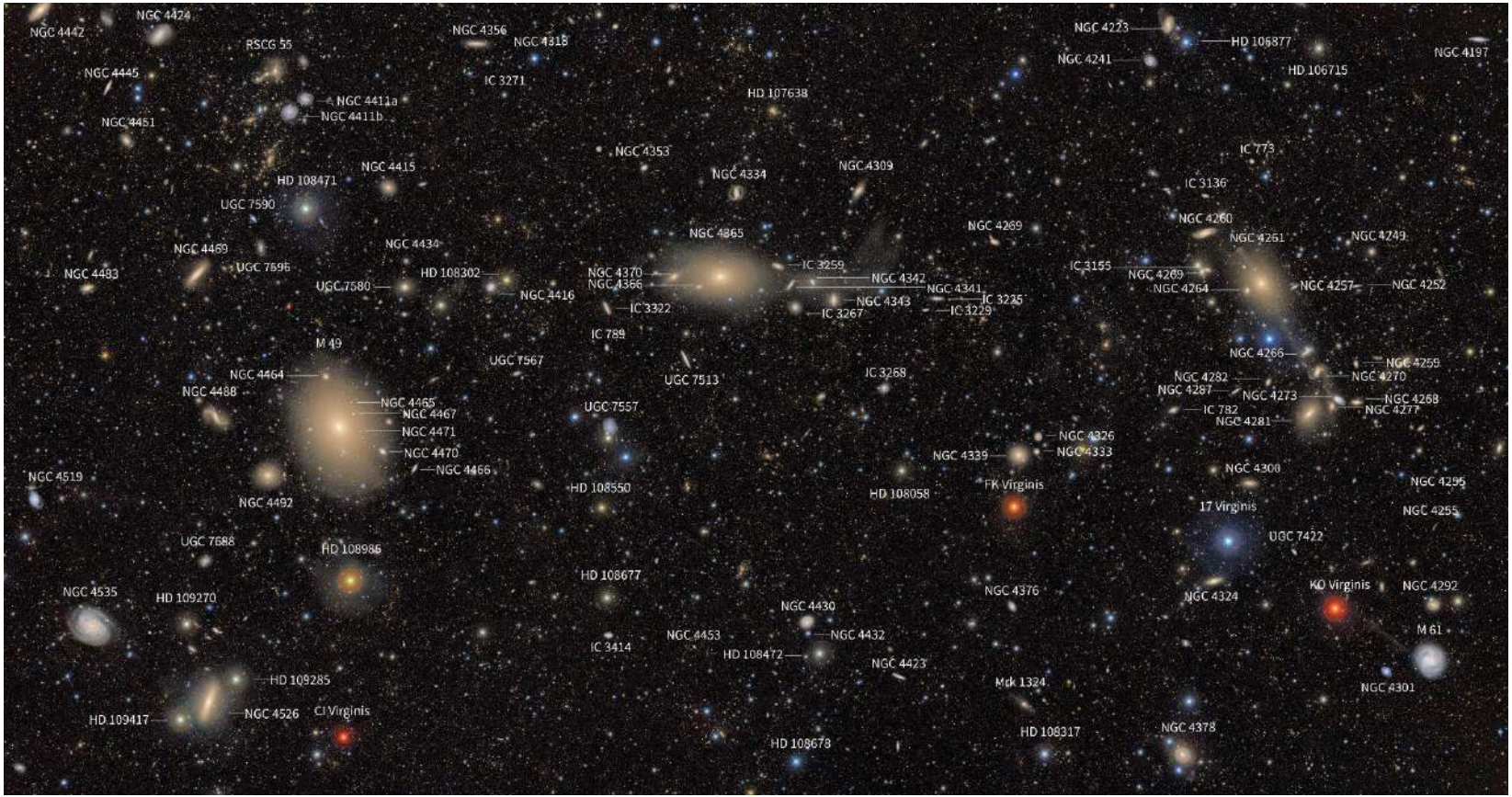




Outline

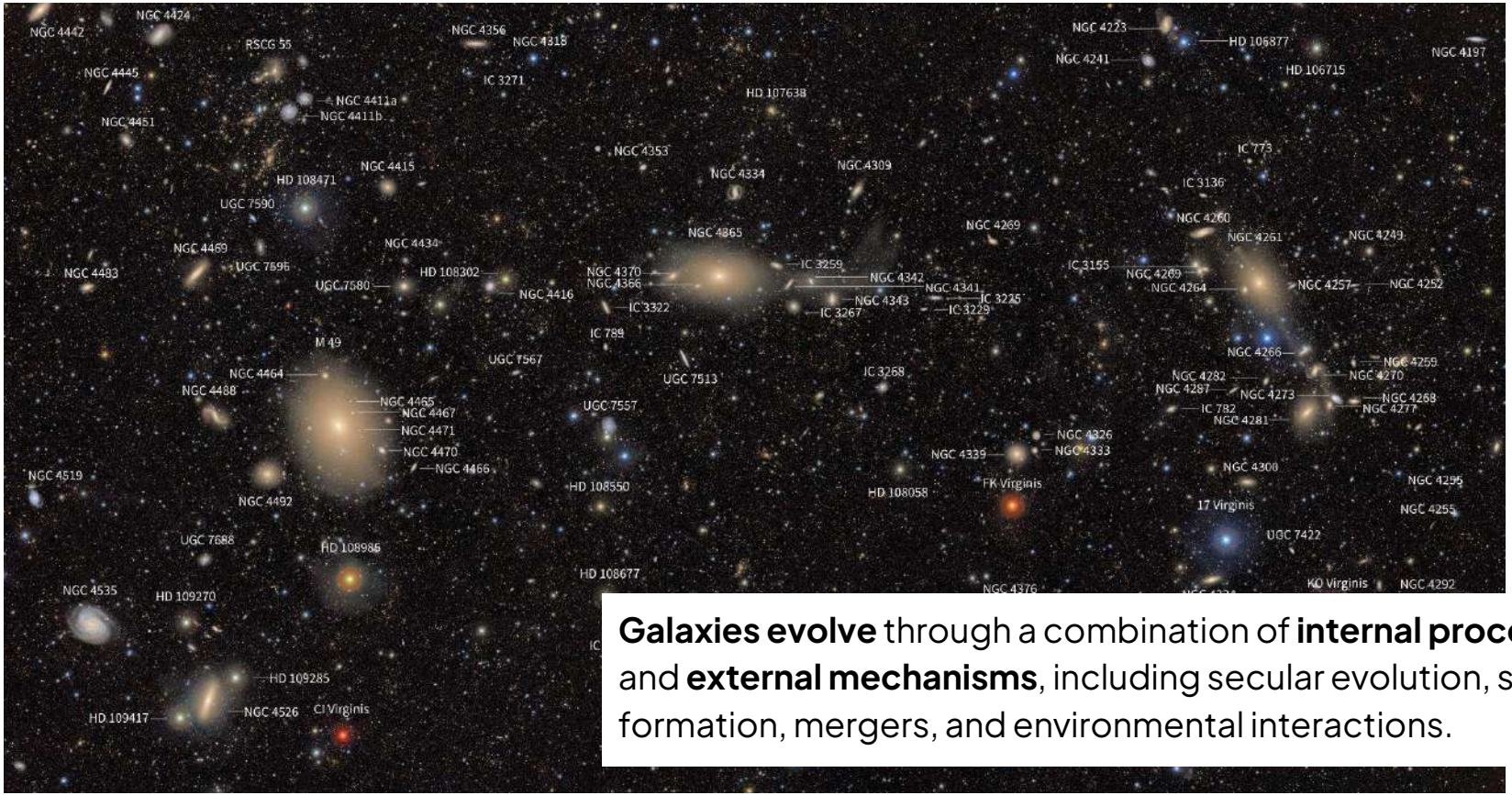
- Motivation
- Part I: Detecting Globular clusters in deep and wide area Survey
- Part II: NGC 1527 – a test case with DP2
- Other projects & Summary

Motivation – Virgo Galaxy Cluster – Vera Rubin Observatory



Credit: RubinObs/NOIRLab/SLAC/NSF/DOE/AURA

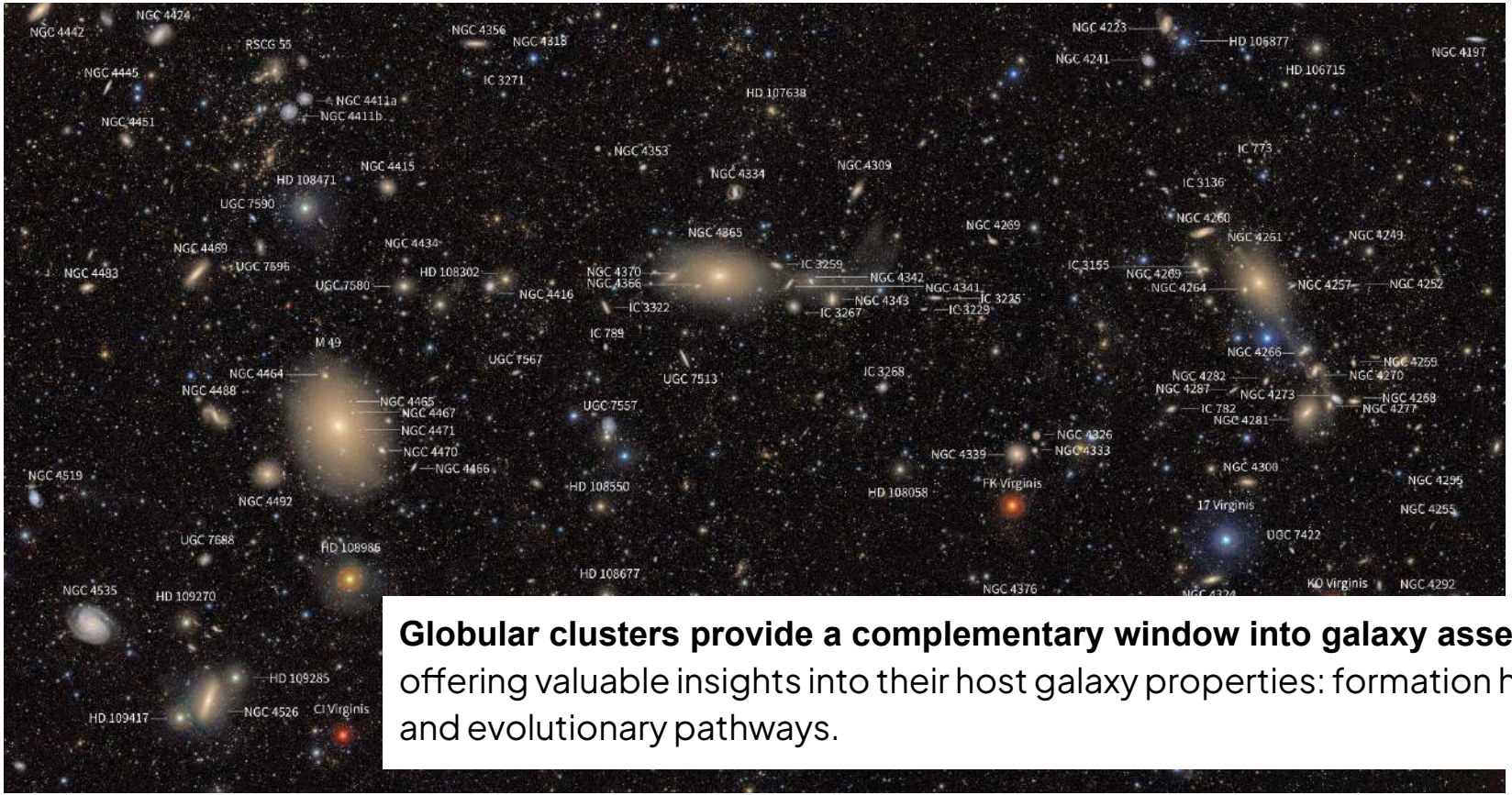
Motivation – Galaxy Mass Assembly History



Galaxies evolve through a combination of **internal processes** and **external mechanisms**, including secular evolution, star formation, mergers, and environmental interactions.

Credit: RubinObs/NOIRLab/SLAC/NSF/DOE/AURA

Motivation – Galaxy Mass Assembly History



Globular clusters provide a complementary window into galaxy assembly, offering valuable insights into their host galaxy properties: formation histories and evolutionary pathways.

Credit: RubinObs/NOIRLab/SLAC/NSF/DOE/AURA

Motivation – GC's Key Properties

- High stellar density: stars are concentrated in a compact volume, making GCs dynamically distinct from diffuse stellar systems.
- Old ages: they preserve information about early stages of galaxy formation.
- Low metallicities in many clusters: their chemical abundances provide clues to the conditions in which they formed.

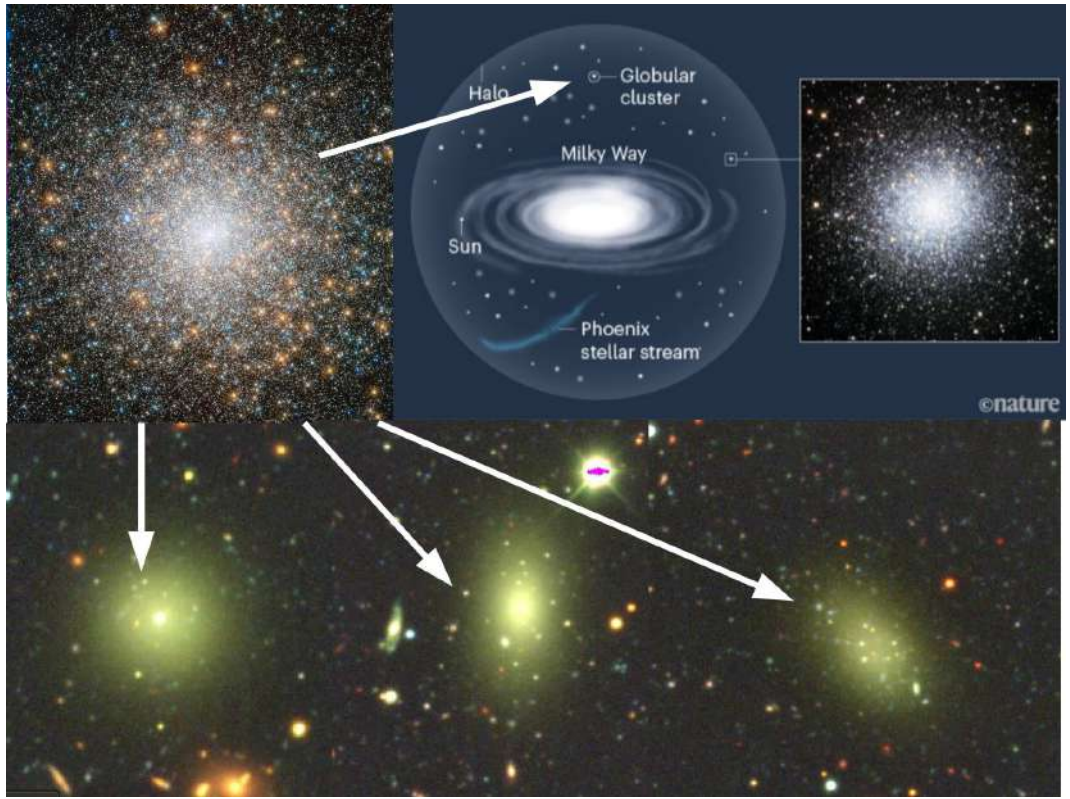

NGC 6441, GC from MW
Credits: Hubble/ESA and NASA, G. Piotto

- Long dynamical survival: many have survived for billions of years, despite tidal forces, stellar evolution, and dynamical interactions.
- Broad spatial distributions: GC systems can extend far beyond the visible stellar bodies of their host galaxies.

e.g. Peng 2006, Yoon+2006, Leaman+2013, Zinn+1985, Brodie+2006

Motivation – Extragalactic Globular Clusters

Extragalactic Globular Clusters are seen as point sources, although enclosing the mass of 10^5 – 10^6 stars.

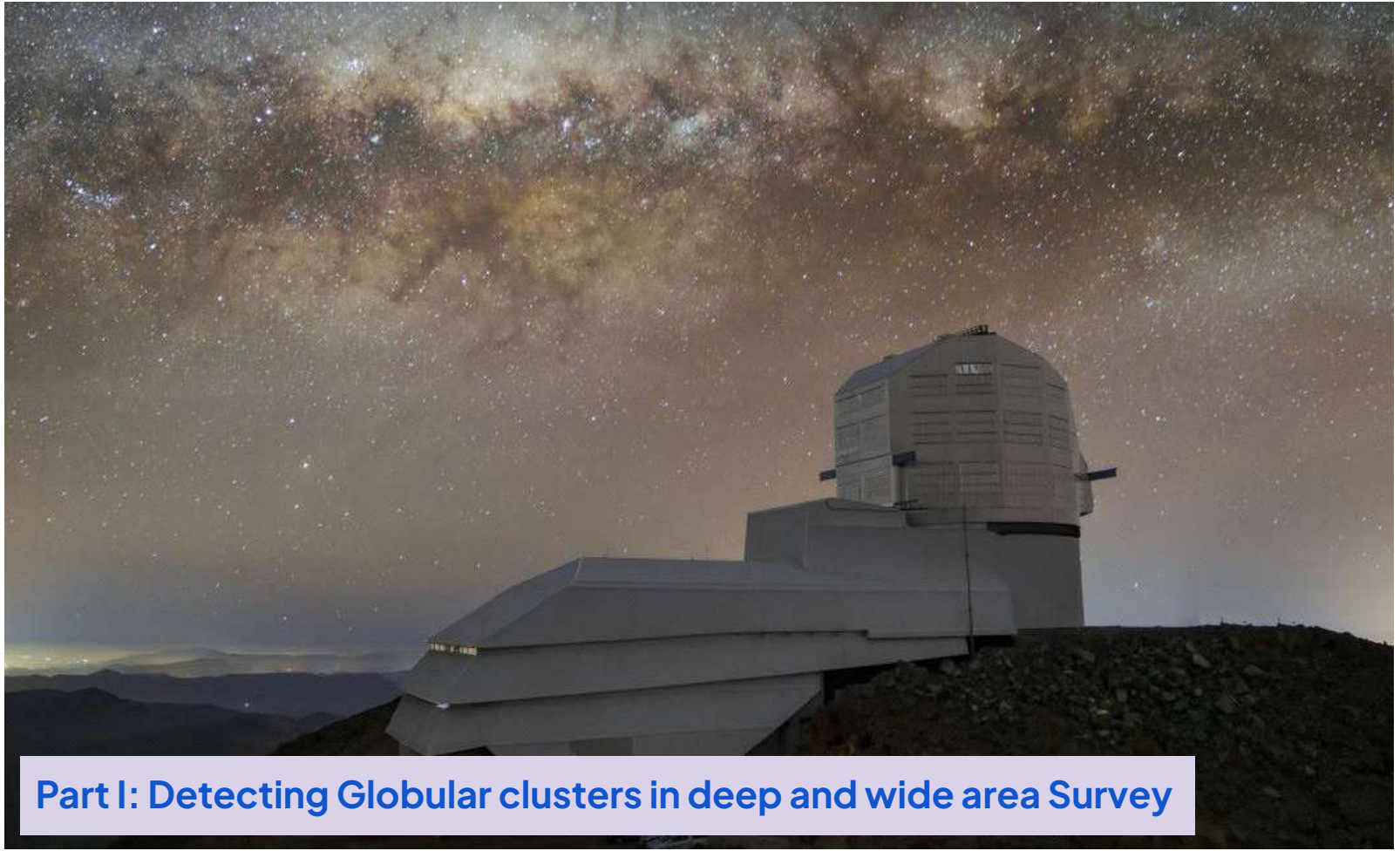


GC system (total GCs in a galaxy)

Their properties are closely linked to those of their host galaxies

e.g. The total mass and number of GCs exhibit a strong connection with the mass of their host dark matter halos

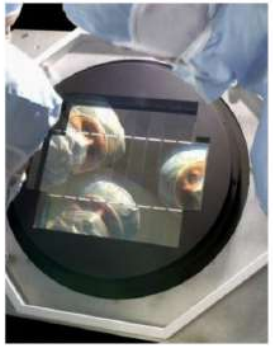
—> making GC systems powerful tracers of galaxy–halo connections.

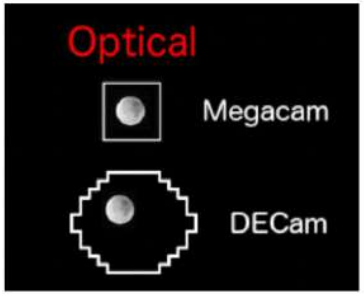


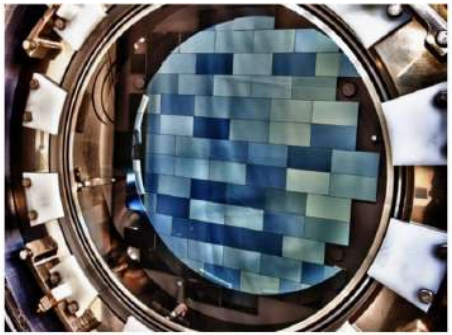
Part I: Detecting Globular clusters in deep and wide area Survey

Large Cameras: Expanding the spatial coverage & resolution

MegaCam
Detectors:
40, 2048 x 4612 pix.
378 megapixels
1 x 1 square degree





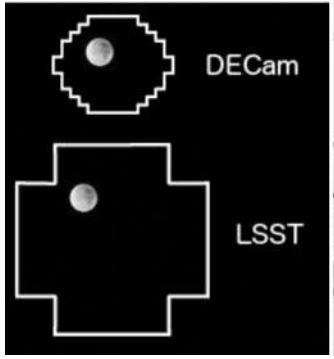


Dark Energy Camera
3 square degree (2.2 degree FoV)
Pixel scale: 0.2637 arcsec/pixel
Detector : 62, 2048x4096 pixel
520 megapixels total



VIRCam
1.64 square degree
Pixel scale: 0.339 arcsec/pixel
Detector : 16, 2048x4096 pixel
64 megapixels total

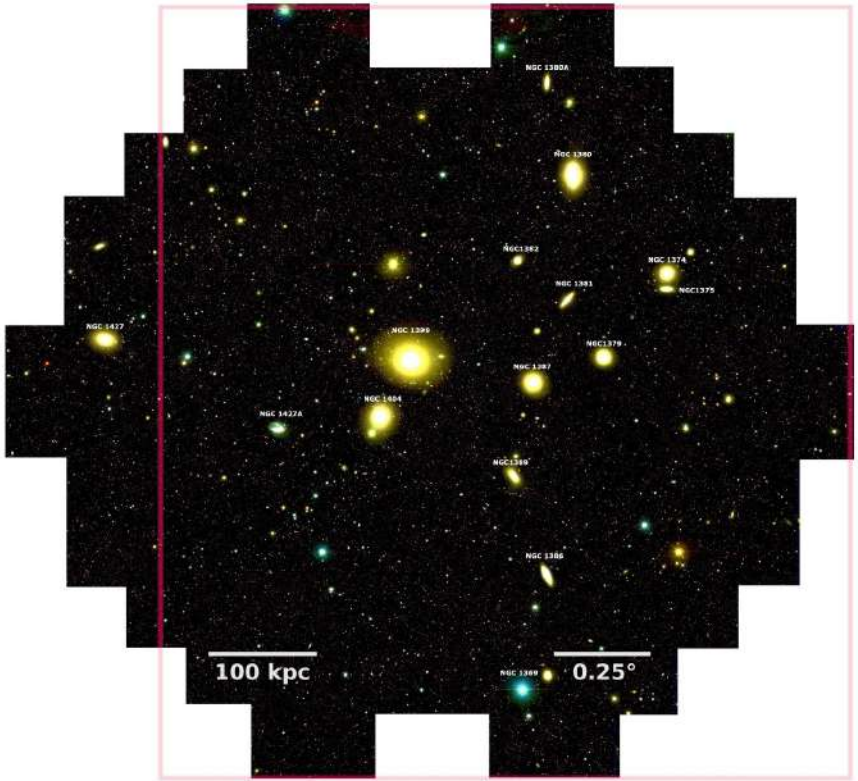






Vera Rubin Observatory, LSST Camera
9.6 square-degree Field of View.
Pixel scale: 0.2 arcsec/pixel
Detector: 189, 4000x4000 pixels
3200 megapixels total

Part I.a: Detecting Globular clusters in deep and wide area Survey – Fornax Galaxy Cluster



Ordenes-Briceño et al. 2026

Example of a study with extended spatial coverage and Multiwavelength.

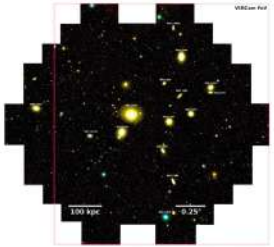
Second closest galaxy overdensity after Virgo
Distance = 19.3 ± 0.7 Mpc (Gagandeep et al. 2024)
Mass = 7×10^{13} $M_{\odot}$

Next Generation Fornax Survey
Central region: 2.6°x 2.6° (1 DECam Tile)
5 filter information:
ugi (DECam) - optical
JKs (VIRCam) - Near Infrared
(the total survey has 19 tiles coverage ~1.3 x R_{viral})

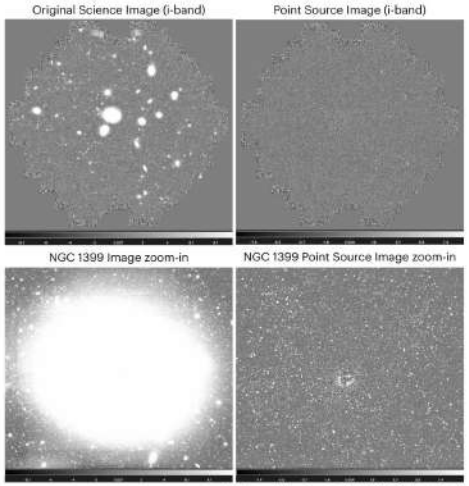
DECam Fov - RGB image (ugi).
VIRCam stack FoV - Red rectangle (JKs)

Detecting Point Sources & Deep color–color diagrams

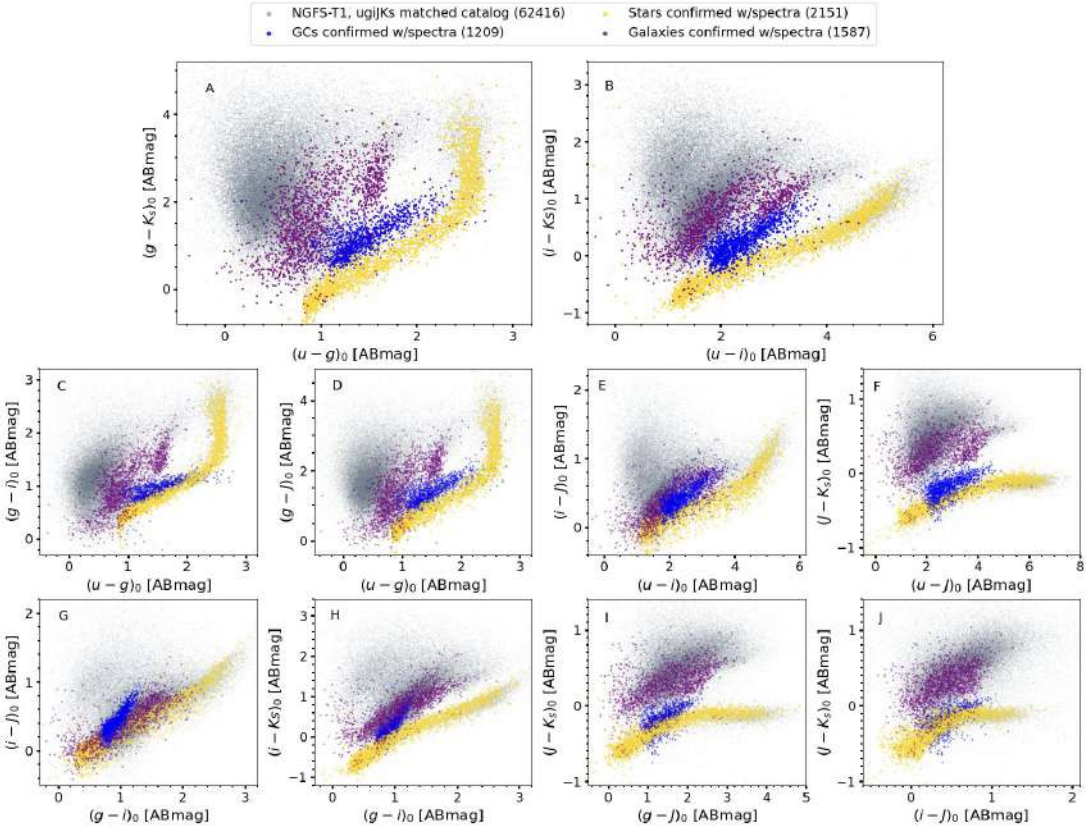
Ordenes-Briceño et al. 2026
A support vector machine approach to disentangling globular clusters.



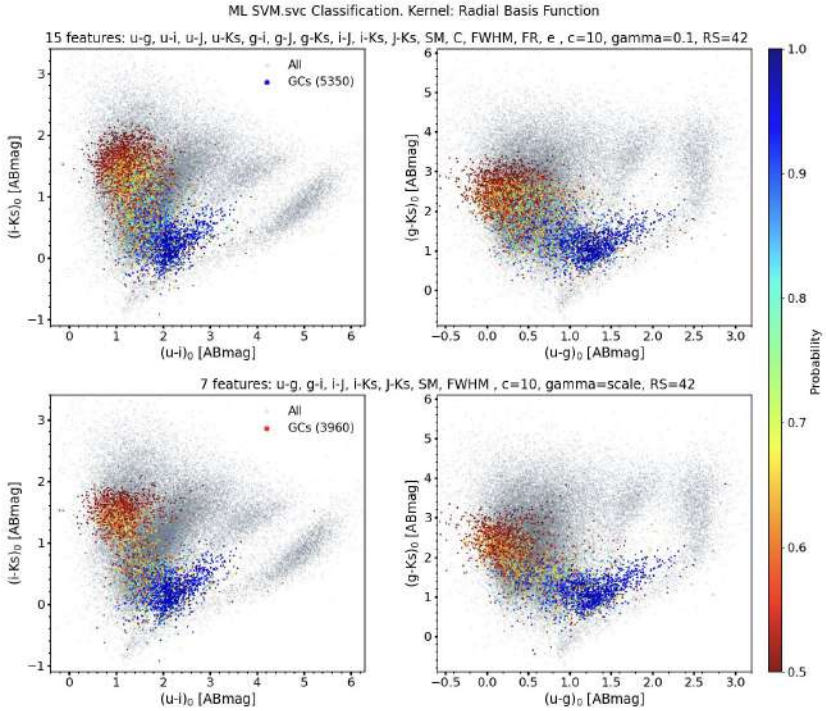
Only for detection - catalog is the initial input for extracting photometry.



Filters: u,g,i,J,Ks



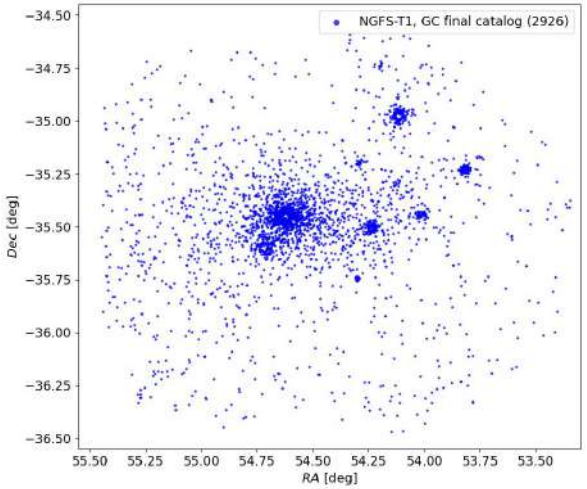
GC selection – Machine Learning Method: Support Vector Machine



Support vector classification (SVM.svc model)

Ordenes-Briceño et al. 2026

- **Classes** (radial velocity confirmed objects compiled from the literature):
  - GCs (blue)
  - Foreground stars (yellow)
  - Galaxies (purple)
- **Kernels:** Radial basis function (C, gamma)
- **Features:** Using available colors with 5 filter combinations and some morphology parameters.

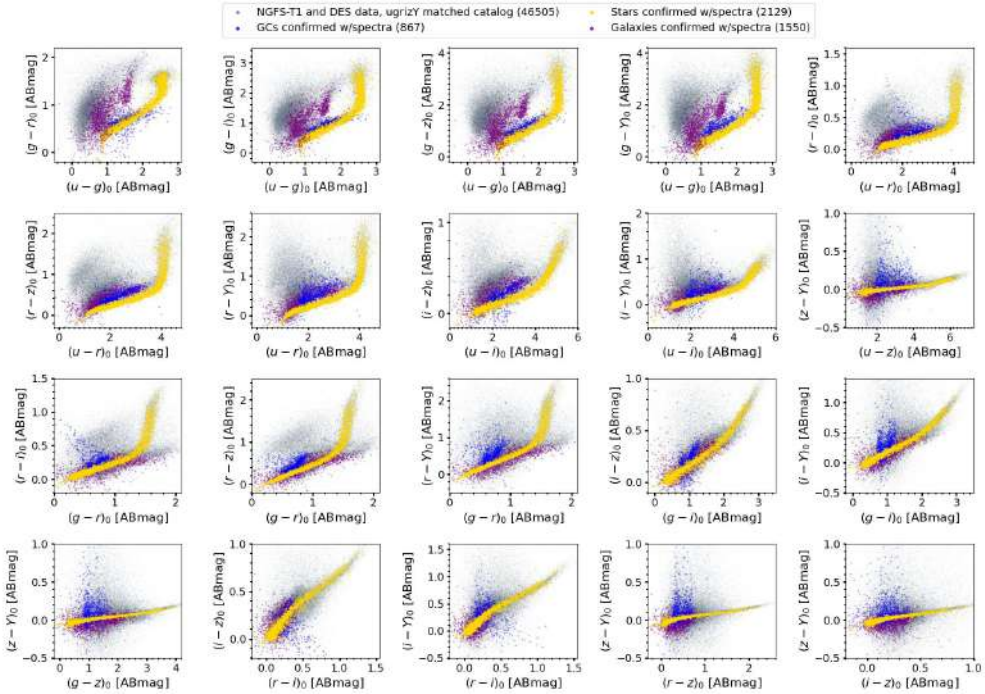


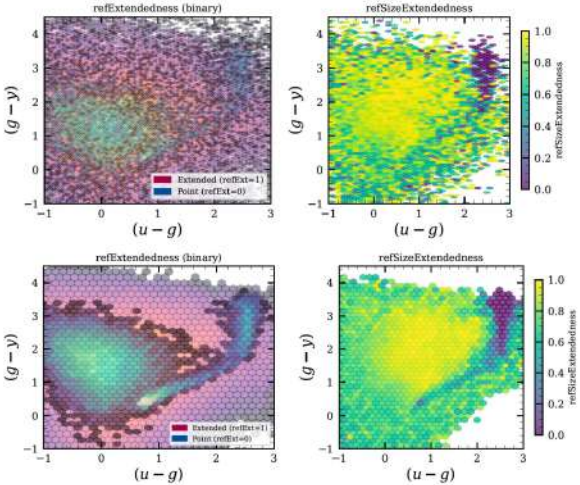
Adopted: 7 feature model (most informative, least correlated features).
96.6% accuracy and misclassifications: 10.4%.
2926 sources SVM selection (1717, prob >80%) + Spect. confirmed (1209)

Part I.b: Detecting GCs in deep and wide area Survey – Rubin DP2 DATA

Plazas Malagón & Ordenes-Briceño et al. 2026

Multi-method Machine Learning classification of astronomical sources with Rubin Data Previews: A spectroscopy free approach with DP1 and DP2





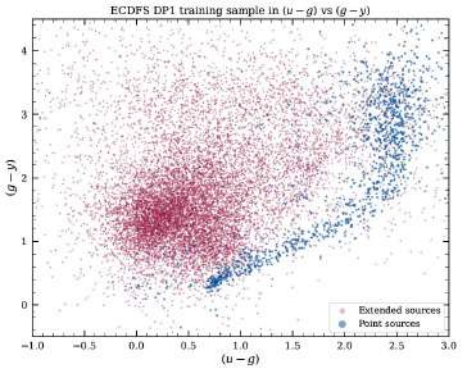
Plazas Malagón & Ordenes-Briceño et al. 2026

NGFS (ugi)+DES DR2 (rzy) : color-color diagrams
Ordenes-Briceño et al. 2026

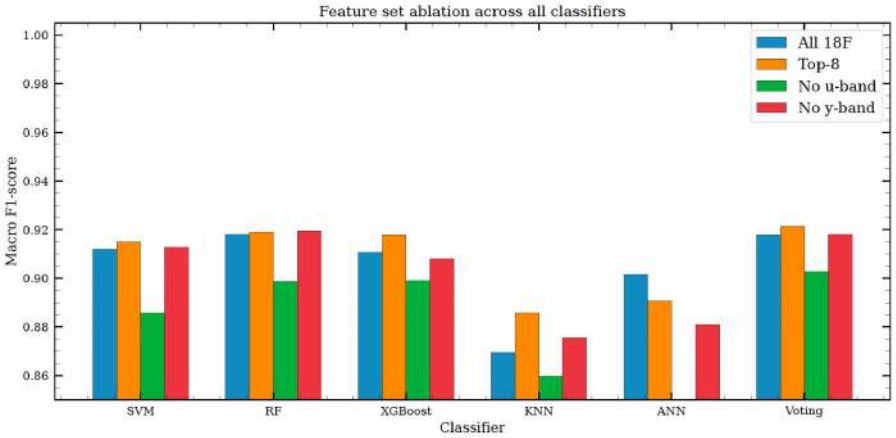
Part I.b: Detecting GCs in deep and wide area Survey – Rubin DP2 DATA

Multi-method Machine Learning classification of astronomical sources with Rubin Data Previews: A spectroscopy free approach with DP1 and DP2

Plazas Malagón & Ordenes-Briceño et al. 2026



- Training/Test sample - Monster catalog (stars) + Photo-z DP1, DP2 available (galaxies)
- Classification between point sources (stars + GCs) and extended sources (galaxies).
- Features: 18 features (15 colors + 3 morphology descriptors), top-8 (the most important 8F by avg. permutation importance),



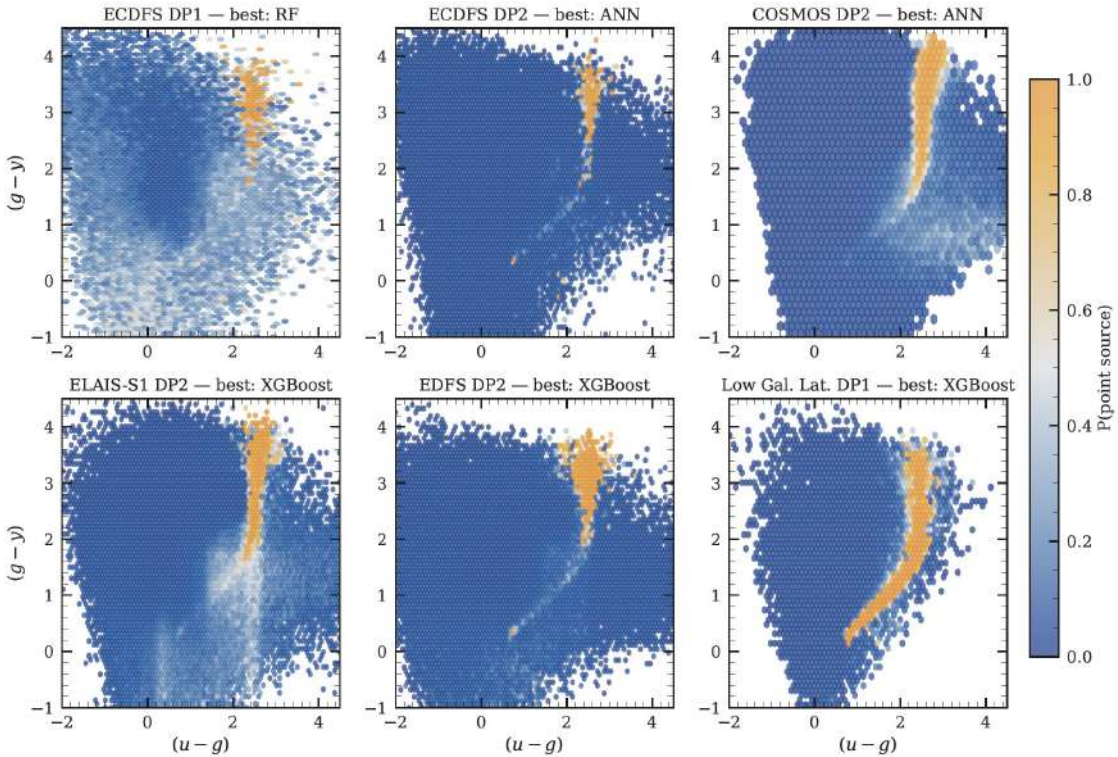
No u-band (13F, no colors with u-band), No y-band (13F, no colors with y-band)

Six Machine Learning Methods:
SVM, Random Forest, XGBoost, KNN, ANN, Voting

Part I.b: Detecting GCs in deep and wide area Survey – Rubin DP2 DATA

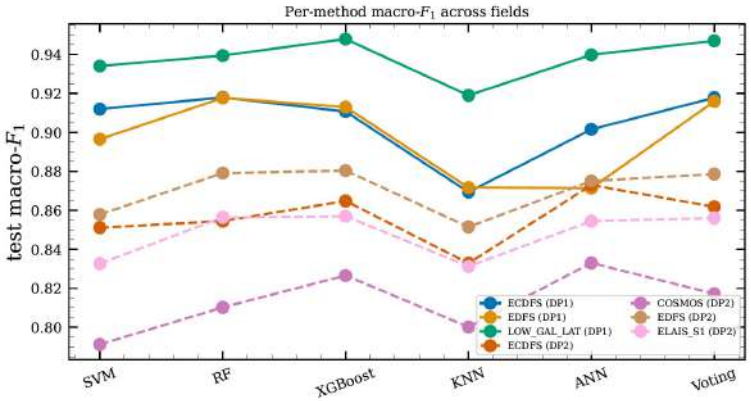
Multi-method Machine Learning classification of astronomical sources with Rubin Data Previews: A spectroscopy free approach with DP1 and DP2

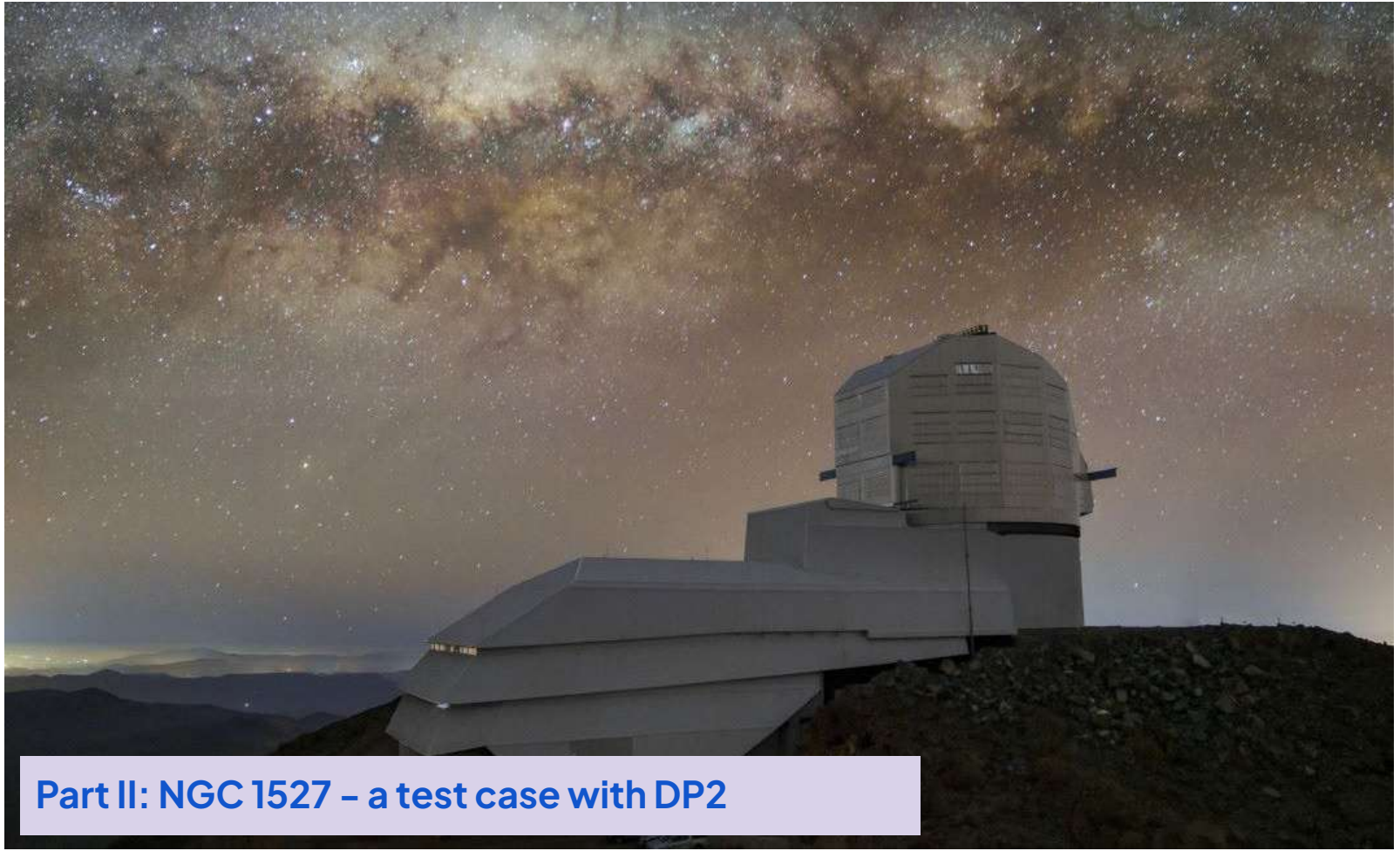
Plazas Malagón & Ordenes-Briceño et al. 2026



The methodology was applied to different LSST fields:

ECDFS DP1,DP2; EDFSb DP1, DP2; Low Gal. Lat. DP1; COSMOS DP2; ELAIS_S1 DP2.

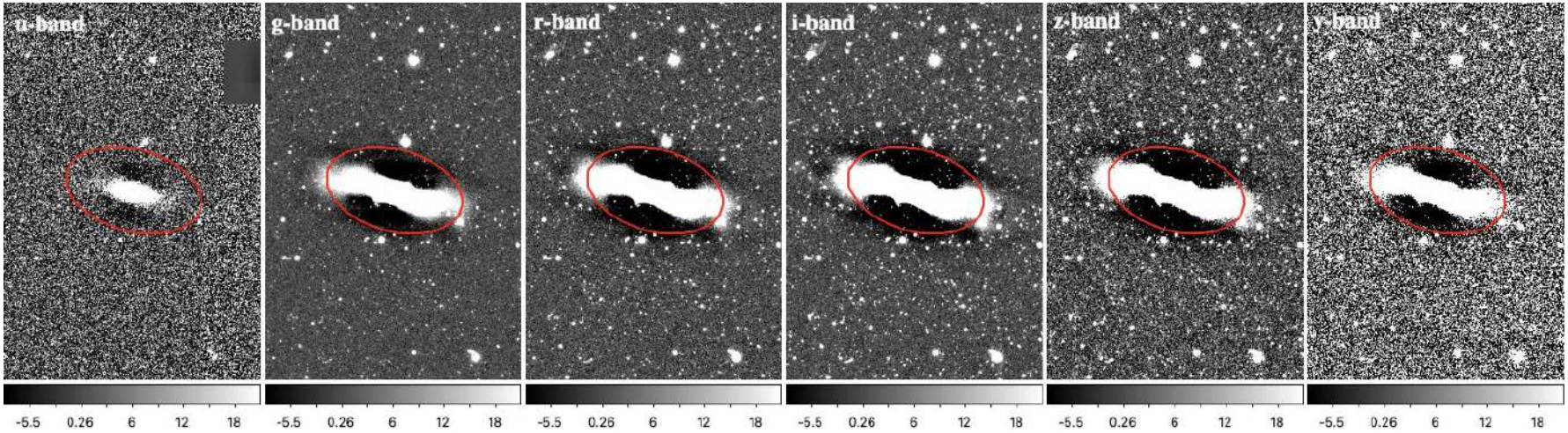




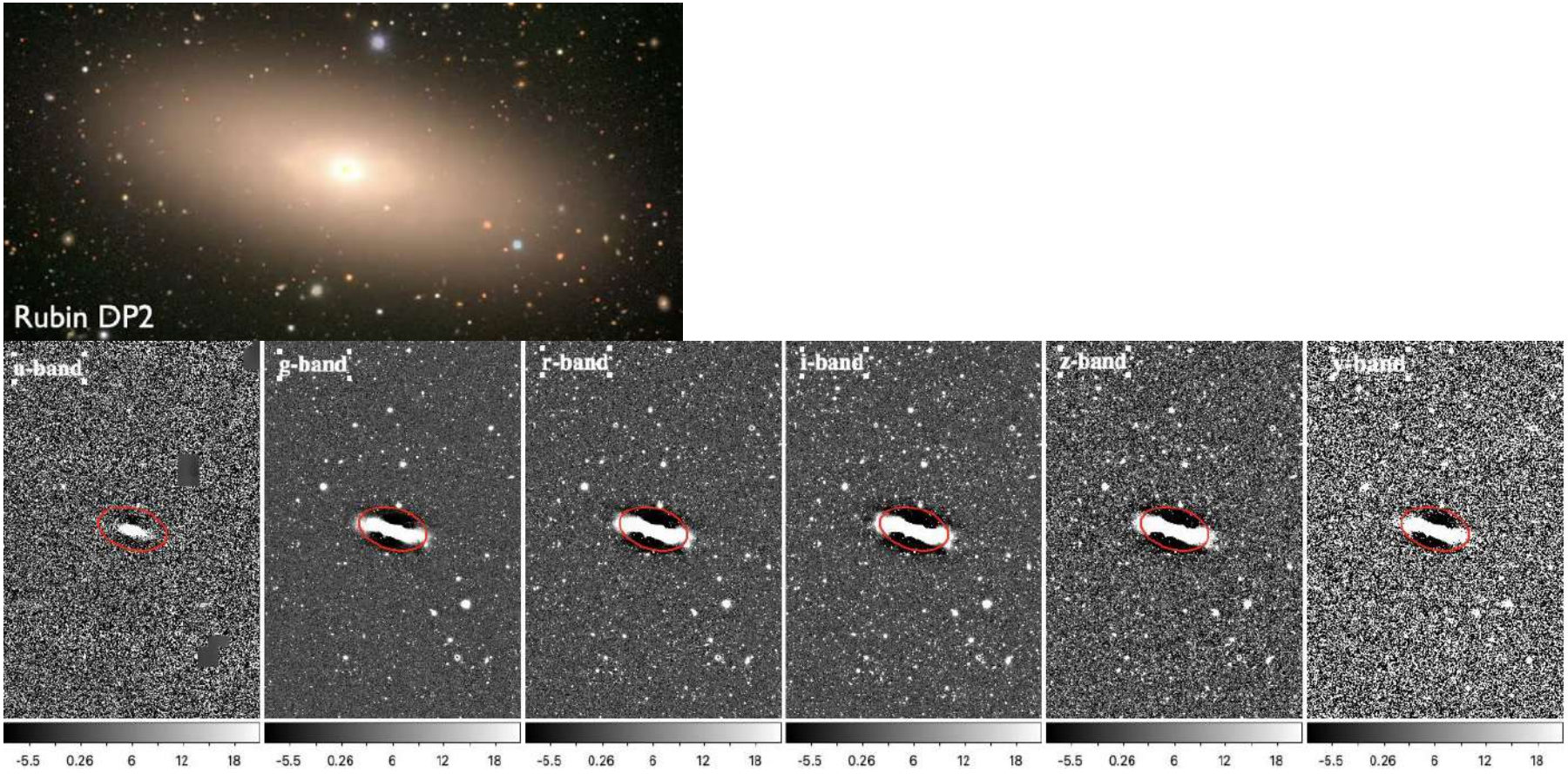
Part II: NGC 1527 – a test case with DP2

Part II: NGC 1527 – a test case with DP2





Part II: NGC 1527 – a test case with DP2





Other projects

Searching for Dwarf Galaxies

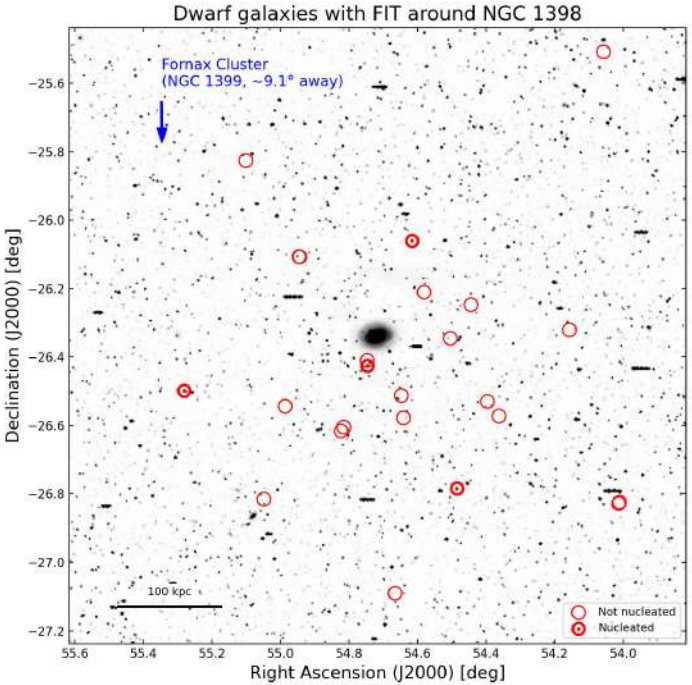
Project: "Exploration of the environment of galaxy NGC 1398 with a multi-wavelength approach" López-Echeverri et al. *in prep.*

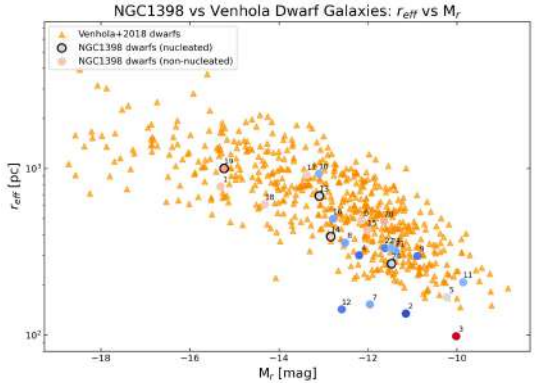


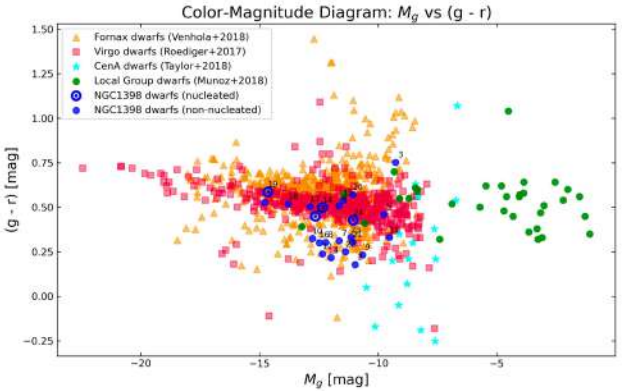
Andrés López-Echeverri
(BSc, University Antioquia, Medellín).

RECA
Red Estudiantes Colombianos Astronomia

INTERNSHIP RECA







Adding GC extraction to BUDDI (Bulge–Disc decomposition of IFU data)

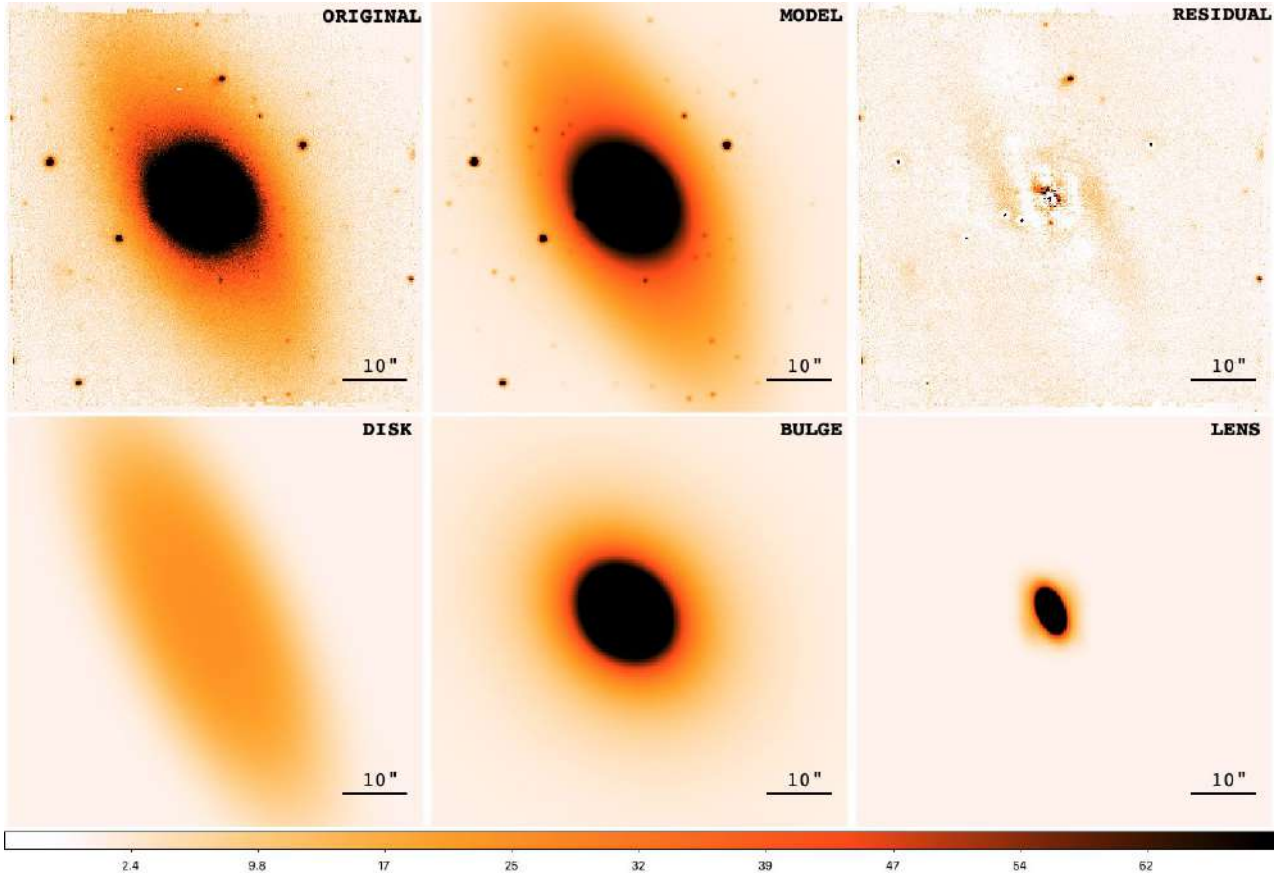
Galaxy test: CCC122
MUSE data

BUDDI Output:

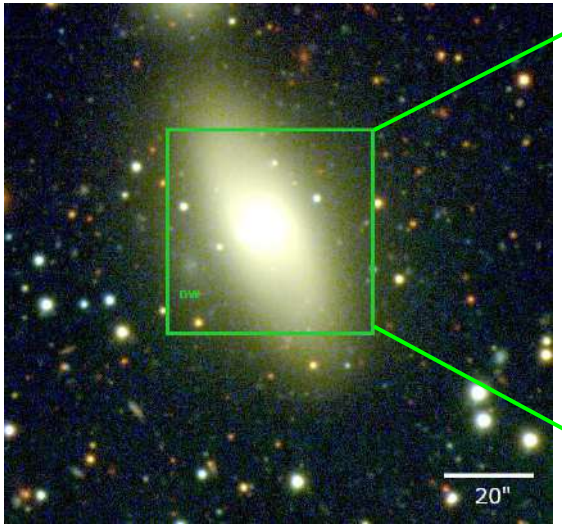
- 3 galaxy components:
- Disc, bulge, lens. Cube - 1D spectra
- Original -Cube
- Best model - Cube
- Residual - Cube

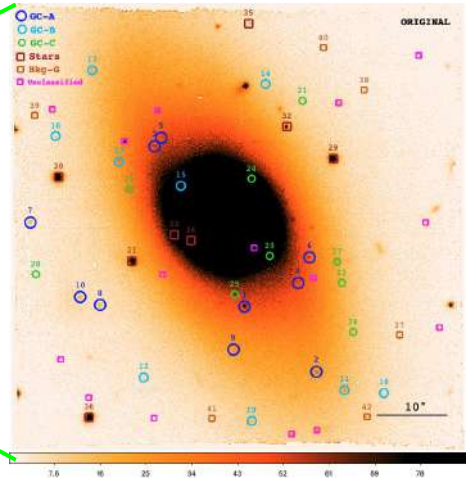
New output
57 psf components
- 1D spectra

Ordenes-Briceño et al. (in prep), to be submitted in November

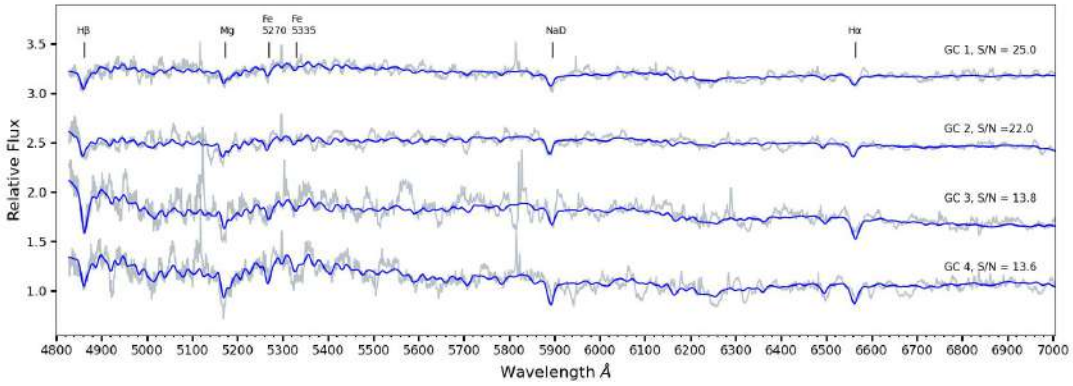


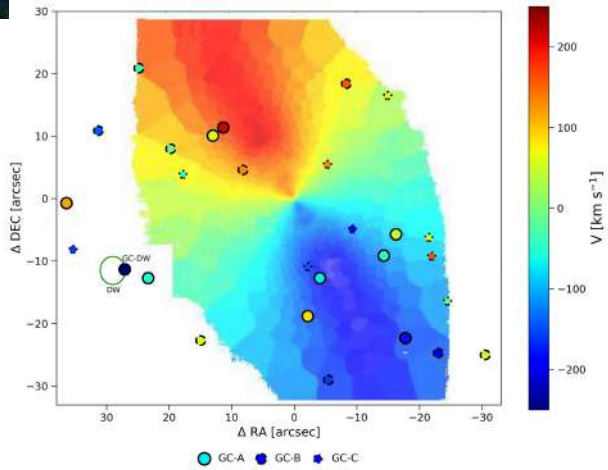
BUDDI-GC
Extraction Results
Test case: CCC122

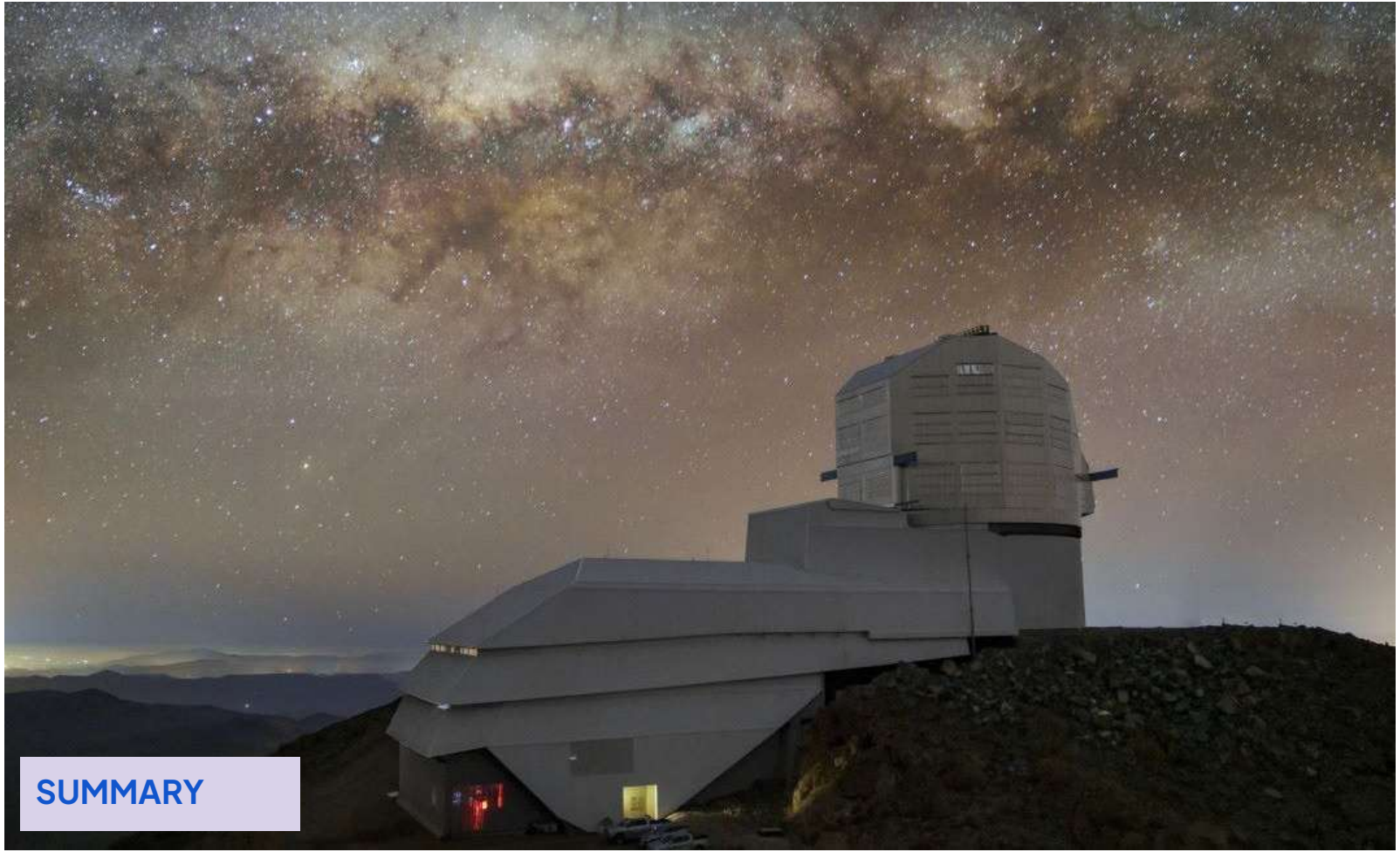




Ordenes-Briceño et al. (in prep), to be submitted in November





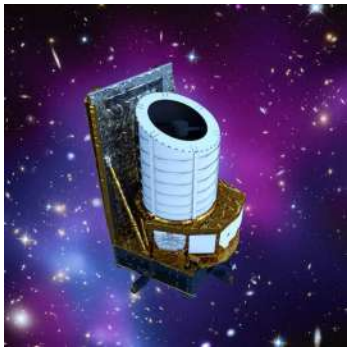


SUMMARY

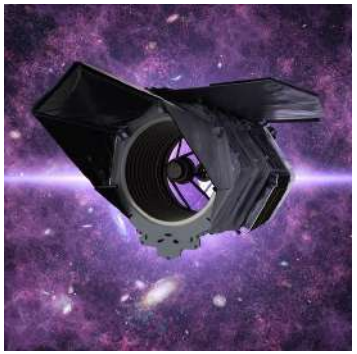
Multi-wavelength Imaging Approach -Powerful synergies



Vera Rubin
Filters: ugrizy



Euclid
Filters: VIS, Y, H, J



Roman Telescope
Filters: RzYJHKs

- Wide-field surveys are/will not just increase the number of known globular clusters. They are making it possible to build more homogeneous, statistically controlled GC catalogs across different galaxy masses and environments.
- This will require more careful treatment of selection effects, contamination, and physical interpretation. Multiwavelength studies + Machine learning methods.
- GCs will keep providing key information about galaxy assembly, halos & dark matter: GC colour distributions, subpopulations, metallicity gradients, and accretion signatures. GC spatial profiles, total GC populations, halo mass relations, and radial extent.
- Spectroscopic follow-up necessary to confirm they belong to the host galaxy system.